Université Paris-Saclay

The nucleus,
a unique many-body system

Elias KHAN
IJCLab - Orsay
IN2P3 - CNRS

Foreword

The nucleus is the only many-body system in Nature where all the following conditions are fulfilled: i) all four fundamental interactions are involved; ii) its constituent (the nucleon) is non-elementary and iii) it is of finite-size. The conjunction of these 3 features is the root of the tremendous richness of the nuclear phenomenology. On the other hand, nuclei are systems difficult to describe accurately.

The nucleus is also involved in important processes of Nature such as the five main types of nucleosynthesis in the Universe, or natural radioactivities surrounding us.

This introductory nuclear physics course proposes a modern way to describe the nucleus, starting from fundamental aspects of many-body system and leading to an universal approach of the various nuclear states. Modern views on the nuclear interaction and radioactivities are also provided. Finally an overview of astrophysical sites involving nuclei is given.

Index

Chapter 1

Dimensionless study of many-body systems

Dimensionless quantities are well designed to perform an universal study and comparison among various systems. After sketching the general properties of states of matter, the building of relevant dimensionless quantities is undertaken in this chapter.

1.1 States of matter

When temperature decreases and density increases, a system of constituents interacting with a short range attractive interaction undergoes from a classical gaseous state to a liquid one. When further decreasing the temperature and increasing the density, the system becomes a solid, which is microscopically described as a crystal structure. Microscopically, the system went from weakly interacting constituents (gas) towards more interacting ones (liquid) to bound states into crystal having constituents fixed at periodic nodes (solid).

What happens if the density further increases, that is adding constituents between the nodes of the crystal ? In this case, the constituents at the nodes start to overlap, forming a molecule of constituents, and the system becomes clusterised. When the density further increases, the dense system becomes homogeneous and this is the quantum liquid state where the constituent wavefunction is strongly delocalised. If the density increases again, the inner structure of the constituents starts to impact, and the system cannot only be considered of interacting constituents anymore.

The main states of matter can be ordered in the diagram depicted on Fig. 1.1.

1.2 Three quantities

The information of an interacting many-body system can be reduced to 3 basic quantities: the typical magnitude -V'$_0$ (V'$_0$>0) of the attractive two body interaction, it's typical range r_0 in the system and the mass m_N of each interacting particle. An example of interaction between two nucleons is given in Fig. 1.2.

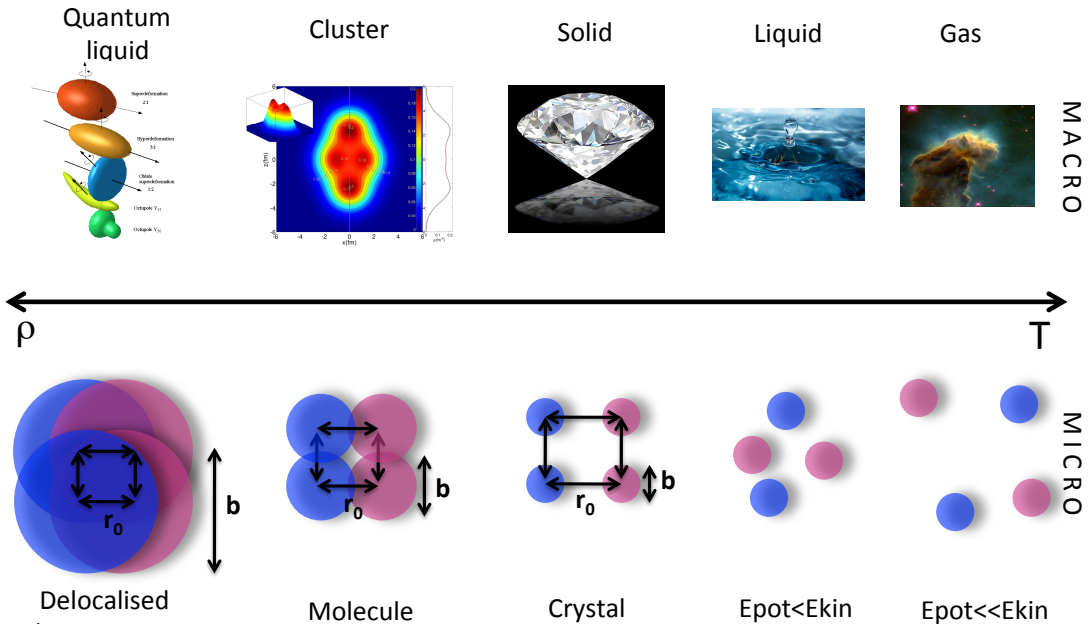

Figure 1.1: Summary picture of the matter states. ρ is the density of the system and T its temperature.

It should be noted that the equation of motion (the Schrödinger or the Dirac one) is nothing but the use of these 3 quantities in the most updated way in order to predict the relevant state of the system. Information extracted from the equation of motion will be used starting from chapter 2.

In order to study universal features of many body systems, a powerful tool is to build dimensionless ratios using V'$_0$, r$_0$ and m$_N$.

1.3 Dimensionless ratios

Among all the possible dimensionless ratios which can be built from V'$_0$, r$_0$ and m$_N$, at least four of them have a specific meaning : the dimensionless coupling constant α, the so-called spin-orbit parameter η, the quantality Λ and the action $\mathcal{A}$.

Two dimensionless ratios, α and η, are enough to characterize the system. Therefore Λ and $\mathcal{A}$ can be deduced from these two quantities, and are discussed in section 1.5.

A first dimensionless ratio that can be defined is

$$\alpha \equiv \frac{V_0' r_0}{\hbar c} \tag{1.1}$$

This quantity only depends on the interaction and not on the constituent. It can be interpreted as the coupling constant of the interaction: in the case of the electromagnetic interaction, Eq. (1.1) gives

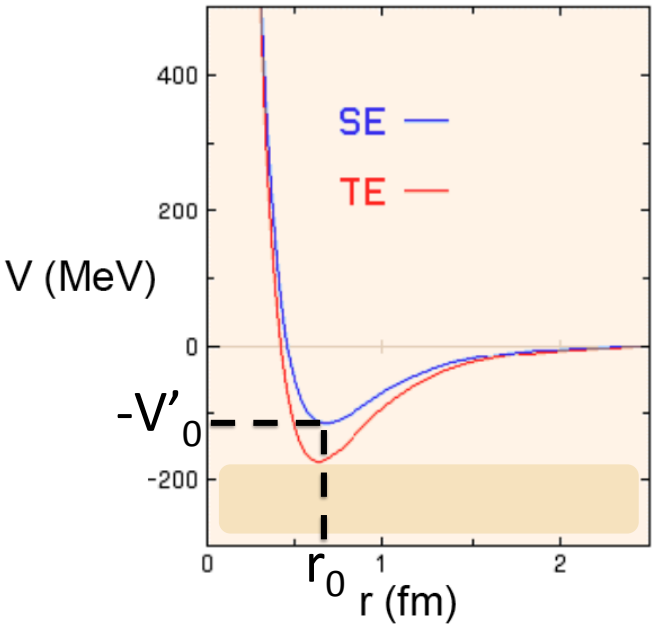

Figure 1.2: The nucleon-nucleon interaction

$$\alpha_{EM} \simeq \frac{e^2}{4\pi\epsilon_0\hbar c} = \frac{1}{137} \tag{1.2}$$

which is the fine structure constant.

In the case of the strong interaction in nuclei, (1.1) gives, as seen from Fig. 1.2,

$$\alpha_S \simeq \frac{100MeV.1fm}{200MeV.fm} \simeq 1 \tag{1.3}$$

which is the typical magnitude of the strong interaction in these systems.

Table 1.1 summarizes the typical value of the coupling constants for the 4 fundamental interactions to be found in Nature.

It should be noted that in addition to the 4 fundamental interactions, the effective interaction can take various coupling constant values in many-body systems, such as in graphene where α=2.5 or in molecular systems where $\alpha \sim 10^{-6}$. It should also be noted that r_0 is the range of the interaction at work in the system. In the electromagnetic case in atoms, r_0 is typically the Bohr radius.

The strong interaction has the largest coupling constant among the 4 fundamental interactions. Its very short range explains why it has not been discovered before the last century whereas the electromagnetic and gravitational ones where known much earlier, although less intense. It should also be noted that the strong interaction drives the microscopic structure of matter: the electromagnetic interaction has the typical magnitude of a perturbation (1/137), compared to the strong

Interaction	Strong	Electromagnetic	Weak	Gravitation
Year of first modelisation	1935	1873	1933	1687
Mediator	gluons / mesons	photon (γ)	$W^{\pm}$, Z^0	graviton ?
Mass	M_g=0 $M_{meson}\sim$ 200 MeV	0	$M_W c^2$ = 80,4 GeV $M_Z c^2$ = 91,2 GeV	0
Source	Color charge	Electrical charge	Weak charge	Mass
Range (m)	$\lesssim 10^{-15}$	∞	10^{-18}	∞
Coupling	$\alpha_S = g_S^2/4\pi\hbar c \leq 1$ ~ 1 ($r \sim fm$) < 1 ($r \ll fm$)	$\alpha = e^2/4\pi\varepsilon_0\hbar c$ = 1/137	$\alpha_W = g_W^2/4\pi\hbar c$ $\sim 10^{-6}$	$G_N M^2/4\pi\hbar c$ $= 5 \times 10^{-40}$

Table 1.1: Summary of the main features of the 4 fundamental interactions to be found in Nature.

interaction. The noticeable fact that α is around 1 in the case of the strong interaction promotes the fine structure constant as the direct ratio of the magnitude of these two interactions. However, historically the fine structure constant was introduced to measure the typical spin-orbit splitting in atoms (which behaves as α_{EM}^2, which is very small compared to 1). It shall be shown in chapter 2 that a more general quantity drives the spin-orbit effect in many-body systems. This is connected to the spin-orbit parameter.

1.4 The spin-orbit parameter

The second relevant dimensionless ratio is the so-called spin-orbit (LS) parameter η defined as

$$\eta \equiv \frac{m_N c^2}{V_0'} \tag{1.4}$$

It is another dimensionless ratio which can be built from V'$_0$, r$_0$ and m$_N$. Formally, α and η form the complete set of dimensionless ratios which can built from the 3 main quantities of a many-body system. More complicated dimensionless ratios can be built, such as the quantality and the action, but they can always be expressed from α and η (see section 1.5).

If the typical kinetic energy T$_N$ of a constituent is approximated to V'$_0$ then η measures the relativistic effects at work in the system: it is non-relativistic when η goes to infinity, relativistic when η is close to 1, and ultra-relativistic when η goes to 0.

It will been shown in chapter 2 that in finite systems, η also drives the relative magnitude of the spin-orbit effect not only in atoms but also in other fermionic systems such as nuclei, hypernuclei and quarkonia.

1.5 Action and quantality

Two related and physically useful quantities can be built from η and α: the action $\mathcal{A}$ and the quantality Λ.

The action of the system, normalised to $\hbar$, is

$$\mathcal{A} \equiv \frac{r_0 \cdot \sqrt{m_N . V_0'}}{\hbar} = \alpha\sqrt{\eta} \tag{1.5}$$

It is well known that quantum effects in a system are large when its action is close to $\hbar$, as it can be induced from the Heisenberg relations.

The quantality Λ is defined as the ratio of the zero point kinetic energy T_0 to the magnitude of the interaction V'_0:

$$\Lambda \equiv \frac{T_0}{V_0'} \simeq \frac{\hbar^2}{m_N r_0^2 V_0'} = \frac{1}{\eta\alpha^2} \tag{1.6}$$

It is also built from V'_0, m_0 and m_N. It should be noted that if the typical kinetic energy of a constituent T_N is approximated to V'_0, then Λ is the ratio of the zero point kinetic energy T_0 to T_N.

The quantality carries similar information than $\mathcal{A}$, the action of the system normalised to $\hbar$: Eqs (1.6) and (1.5) yield

$$\Lambda = \frac{1}{\mathcal{A}^2} \tag{1.7}$$

Both action and quantality can be used to describe when a system behaves like a quantum liquid (QL) rather than a crystal. Large quantum effects in a system (action close to $\hbar$) correspond to $\mathcal{A} \gtrsim 1$ and $\Lambda \lesssim 1$. This is the quantum liquid case. When quantum effects are smaller, such as in the crystal case, the action of the system is significantly larger than $\hbar$: $\mathcal{A} \gg 1$ and therefore $\Lambda \ll 1$: the present use of the quantality and the action is relevant in order to analyse the quantum liquid (QL) or crystal behavior of the system.

Table 1.2 shows the typical quantality values for various systems. Λ is large for QL states and small for crystal ones. The typical value calculated with Eq. (1.6) is $\Lambda \simeq 10^{-2,-3}$ in the case of crystals like atoms and molecules, and $\Lambda \simeq$ 0.1-1 in the case of QL such as ^{4}He, nuclei or electrons in atoms. In the case of nuclei $\Lambda \simeq 0.5$, using $V'_0 \simeq 100$ MeV and $r_0 \simeq 1$ fm. They therefore behave like quantum liquids and nucleon's wavefunctions have a large delocalisation.

Table 1.2: Effective coupling constant, spin-orbit parameter, action and quantality for various many-body systems. m_N is the constituent mass, given in units of a nucleon mass for convenience.

Constituent	m_N	r_0 (nm)	V'$_0$ (eV)	α	η	$\mathcal{A}$	Λ	State
^{20}Ne	20	0.31	31 10^{-4}	4.9 10^{-6}	6.1 10^{12}	12.0	0.007	crystal
H_2	2	0.33	32 10^{-4}	5.3 10^{-6}	5.9 10^{11}	4.1	0.06	crystal
^{4}He	4	0.29	8.6 10^{-4}	1.2 10^{-6}	4.4 10^{12}	2.7	0.14	QL
^{3}He	3	0.29	8.6 10^{-4}	1.2 10^{-6}	3.2 10^{12}	2.3	0.19	QL
Nucleon	1	9 10^{-7}	100 10^6	0.46	9.4	1.4	0.5	QL
e^- in atoms	5 10^{-4}	0.05	10	2.5 10^{-3}	5 10^4	0.6	3.1	QL

Chapter 2

Finite systems

In the case of finite systems, two effects are in order: i) the spin-orbit term can be non-negligible and ii) surface effect can occur, whereas the coupling constant (1.1) and the spin-orbit parameter (1.4) do not depend on any finite system effect. It is therefore necessary to include this effect by a way or another using the equation of motion describing the system.

2.1 Bound systems

In a quantum liquid (QL) system, the mean-field is a good approximation due to the large delocalisation of the constituents' wavefunction. Fig 2.1 depicts the typical lengthscales at work in a many-body system. The left part is the localised (crystal) case whereas the right part is the delocalised (QL) case. In QL it is therefore a good approximation to consider an average mean-field, generated by all the constituents, because each of them feels the potential over the system size, due to its large delocalisation.

As a first approximation, the mean-field potential V is the mean value of the interconstituent interaction V' over the matter density ρ of the system:

$$V(\vec{r}) = \int d\vec{r'} V'(\vec{r}, \vec{r'}) \rho(\vec{r'}) \tag{2.1}$$

V is a one-body potential, only depending of the coordinates and quantum number of one constituent. It should be noted that in quantum mechanics, the interacting constituents can be exchanged before and after the interaction (due to indiscernability). Hence the so-called exchange potential should be added:

$$V(\vec{r}, \vec{r'}) = -V'(\vec{r}, \vec{r'}) \rho(\vec{r}, \vec{r'}) \tag{2.2}$$

which is non-local. In the following only the direct part (2.1) of the potential will be considered.

A convenient approximation for a mean-field confining potential is the harmonic oscillator (HO) one: for any potential V(r) (considering here 1D for convenience), close to the equilibrium position r_m (minimal energy state) of the system:

$$V(r) \simeq V(r_m) + \frac{1}{2} \left. \frac{d^2V}{dr^2} \right|_{r=r_m} .(r - r_m)^2 \tag{2.3}$$

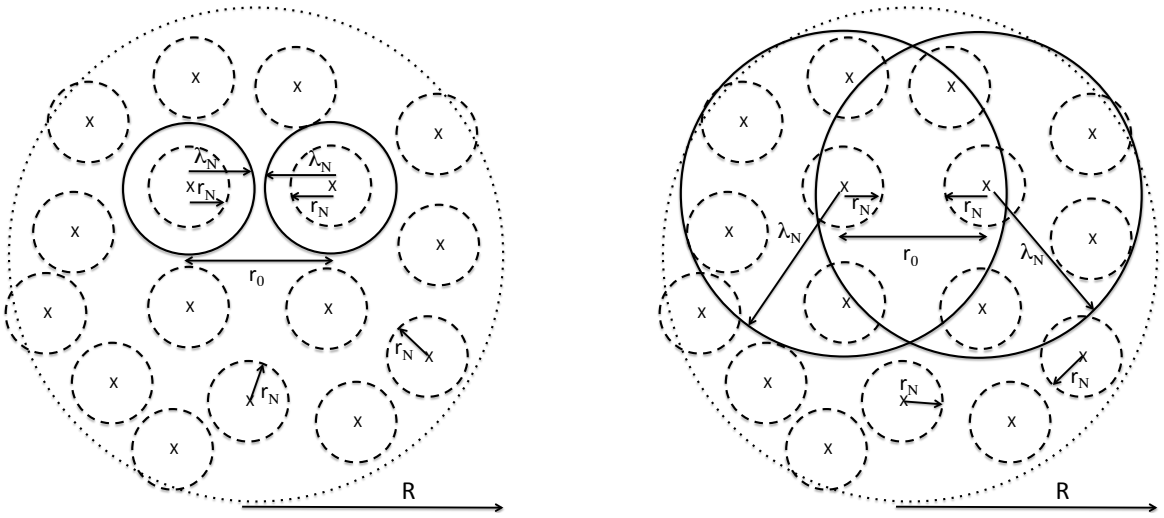

Figure 2.1: Sketch of the various lengthes, in the case of a localised constituent manybody system (left) and in a delocalised one (right). r_N, r_0, λ_N and R are the constituent reduced Compton wavelength, the constituent interdistance, the constituent wavelength and the size of the system, respectively. The constituent wavelength λ_N is displayed for 2 constituents only. The typical spreading of the constituent's wave function follows b $\sim \lambda_N$.

The zeroth order term is a constant, the first order term is zero because of equilibrium, and the third order term is negligible close to equilibrium. Therefore only the second order term matters and Eq. (2.3) is an HO potential: it can be rewritten as

$$V(r) = -V_0 \left[1 - \left(\frac{r}{R}\right)^2\right] \tag{2.4}$$

where V_0 (>0) is the depth of the confining potential and R its radius (see Fig. 2.2). The HO diagonalization (i.e. its solution through a stationary Schrödinger equation) provides discrete energy states. A bound fermionic system therefore automatically exhibits a shell structure corresponding to the degeneracy filling of its states: this is the case for electron in atoms, and also for nucleons in nuclei. Figure 2.2 shows a typical HO potential with its discrete states.

2.2 The spin-orbit effect

The spin-orbit effect can impact on the shell structure. The coupling of the spin of the constituent, with its orbital angular momentum, generates this effect. Intuitively, a particle moving in an electrostatic field generated by another charged particle creates, as a relativistic effect, a magnetic field proportional to its angular momentum. Therefore the interacting energy of this field will follow (ℓ.s) where ℓ is the orbital angular momentum of the constituent and s its spin. The spin-orbit effect adds a term to the central confining potential:

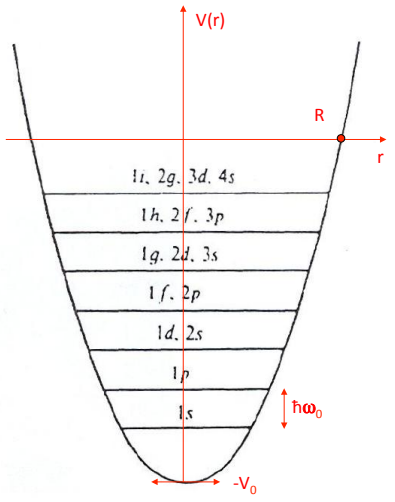

Figure 2.2: The harmonic oscillator potential Eq. (2.4)

$$V_{tot}(r) = V(r) + V_{LS}\vec{\ell}.\vec{s} \tag{2.5}$$

In this case, the whole quantum number labelling of the stationary states has to be rebuilt, because ℓ_z does not commute with the Hamiltonian H anymore. H now commutes with ℓ^2, s^2, j^2 and j_z where the total angular moment j is defined as:

$$\vec{j} = \vec{\ell} + \vec{s} \tag{2.6}$$

This allows to calculate the effect of the spin orbit effect on the energy of the state. One can first show that

$$\vec{\ell}.\vec{s} = \frac{1}{2}(j^2 - \ell^2 - s^2) \tag{2.7}$$

Since j=ℓ+1/2 or j=ℓ-1/2 (because stable subatomic fermions have spin s=1/2), the mean value of the spin-orbit potential is $V_{LS}\hbar^2\ell/2$ or $(\ell+1)V_{LS}\hbar^2/2$, respectively. The spin-orbit potential therefore raises degeneracy, each state being split in two, as depicted on figure 2.3.

The next crucial point is to determine both the value and the sign of V_{LS}, driving the magnitude of the spin-orbit effect. It is small in atoms, but surprisingly, it is large in nuclei. As explained in section 1.4, relativistic effects have to be considered to reach a proper description. It should be noted that in principle V_{LS} of Eq. (2.5) could also depend on the constituent's position coordinate but this will not be considered in the following.

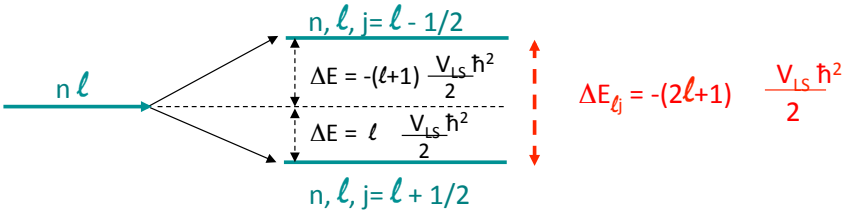

Figure 2.3: The splitting of stationary states of the harmonic oscillator due to the spin-orbit term. The case $V_{LS} < 0$ is considered here.

The Dirac equation

In order to grasp the true origin of the spin-orbit effect, it is necessary to consider the relativistic equation of motion of the constituents in the confining potential. The constituent dynamics is governed by the Dirac equation:

$$\left[\vec{\alpha}\cdot\vec{p}c + U + \beta(m_N c^2 + S)\right]\psi_i = E_i\psi_i \tag{2.8}$$

where ψ_i denotes the Dirac spinor:

$$\begin{pmatrix} \phi_i \\ \chi_i \end{pmatrix} \tag{2.9}$$

for the *i*-th constituent. Because of the Lorentz invariance of the Dirac equation, the potential acting on the nucleon are now of two types: the scalar S(r) one and the vector U(r) one. S(r) has only one component as it is a scalar. U(r) has 4 space-time components, but it is a good approximation to only consider the temporal one which will be labelled U(r) in the following.
In the ground state, A constituents occupy the lowest single-nucleon orbitals, determined by the solution of the Dirac equation (2.8). If one writes the single-constituent energy as $E_i = m_N c^2 + \varepsilon_i$, and rewrites the Dirac equation as a system of two equations for ϕ_i and χ_i, then, noticing that for bound states $\varepsilon_i << m_N c^2$ (this is the case both for electrons in atoms and nucleons),

$$\chi_i \approx \frac{1}{2\mathcal{M}(r)}(\vec{\sigma}\cdot\vec{p}c)\,\phi_i \tag{2.10}$$

to order $\varepsilon_i/m_N c^2$, with

$$\mathcal{M}(r) \equiv m_N c^2 + \frac{1}{2}\left(S(r) - U(r)\right)\ . \tag{2.11}$$

The equation for the upper component ϕ_i of the Dirac spinor reduces to the Schrödinger-like form

$$\left[\vec{p}c\frac{1}{2\mathcal{M}(r)}\vec{p}c + V(r) + V^{LS}(r)\right]\phi_i = \varepsilon_i\phi_i \tag{2.12}$$

for a constituent with effective mass $\mathcal{M}(r)$ in the potential $V(r) \equiv U(r) + S(r)$, and with the spin-orbit potential:

$$V^{LS} \equiv \frac{c^2}{2\mathcal{M}^2(r)}\frac{1}{r}\frac{d}{dr}\left(U(r) - S(r)\right)\vec{\ell}\cdot\vec{s}\,. \tag{2.13}$$

One therefore identifies the confining potential V(r) and the spin-orbit one which are both built from the initial vector U and scalar S Dirac potentials. U and S are generated by the mediators of the interaction (see Chap. 3), therefore the Dirac equation provides a deeper insight in the potentials at work in the system, compared to the Schrödinger one.
It is now possible to derive an evaluation of the magnitude of V_{LS} in various many-body systems.

The spin-orbit rule

In order to evaluate the spin-orbit effect on the shell structure, it is relevant to compare the typical value of the spin-orbit splitting to the major HO energy gap $\hbar\omega_0$. For the harmonic oscillator potential one finds

$$\hbar\omega_0 = \frac{\hbar}{R}\sqrt{\frac{-2V_0}{m_N}}\,, \tag{2.14}$$

where the depth of the potential is $V_0 \equiv V(r=0) = U(0) + S(0)$.
The magnitude of the spin-orbit splitting shall now be evaluated. In both the cases of a short-range interaction (strong interaction) and a 1/r potential (electromagnetic case), the expression for the spin-orbit potential Eq. (2.13) can be rewritten in the following form:

$$V^{LS} \simeq F(r)\,\frac{\rho'(r)}{2\rho(r)r}\,\vec{\ell}\cdot\vec{s}\,, \tag{2.15}$$

where

$$F(r) \equiv \frac{U(r) - S(r)}{\left[m_N c^2 - \frac{1}{2}(U(r) - S(r))\right]^2}\,, \tag{2.16}$$

and ρ(r) denotes the self-consistent ground-state density of a system with A constituents.
For a typical harmonic oscillator approximation, one can show:

$$< \frac{\rho'(r)}{2\rho(r)r} > \simeq -\frac{1}{R^2} \tag{2.17}$$

and, together with $<\vec{\ell}\cdot\vec{s}>= \ell/2$ for $j = \ell + 1/2$, and $<\vec{\ell}\cdot\vec{s}>= -1/2(\ell+1)$ for $j = \ell - 1/2$, the energy spacing between spin-orbit partner states can be approximated by:

$$|\Delta < V^{LS} > | \approx F\frac{\ell(\hbar c)^2}{R^2} \tag{2.18}$$

More precisely, the ratio x between the major energy spacing and the spin-orbit splitting can be written as (using Eqs. (2.14) and (2.18))

$$x \equiv \frac{\hbar\omega_0}{|\Delta < V^{LS} > |} = K\left|\eta - 1 + \frac{1}{4\eta}\right|\,, \tag{2.19}$$

where $K = \sqrt{-2m_N V_0}R/l\hbar$, and

$$\eta \equiv \frac{m_N c^2}{U - S}\,. \tag{2.20}$$

The expression for η is very similar to (1.4). The present expression is more accurate because it is based on the Dirac equation which provides more details about the potentials at work in the system.

K is typically of few units. For instance in the case of nuclei, it is of the order $1 - 5$ for $\ell \geq 3$. Since for the nucleon mass $m_N c^2 \approx 940$ MeV and $U - S \approx 750$ MeV (see section 3.2): $\eta = 1.25$, it follows from Eq. (2.19) that for the nuclear system the ratio x is of the order $1 - 5$, that is, in nuclei, the energy splitting between spin-orbit partner states is comparable in magnitude to the spacings between major oscillator shells. This is because of the near equality of the mass $m_N c^2$ and the potential $U - S$ in nuclei.

In the case of atomic systems the binding of an electron is determined by the Coulomb potential $U(r) = -Z\alpha_{EM}/r$, where Z is the charge of the nucleus and the fine-structure constant $\alpha_{EM} = 1/137$. The energy spacing between successive levels with different principal quantum

number n is proportional to α_{EM}^2, whereas the first-order spin-orbit splitting is $\sim \alpha_{EM}^4$. The ratio between the principal energy spacings and the spin-orbit splittings (fine structure) is much larger than in the nuclear case, that is $\sim 1/\alpha_{EM}^2 \approx 10^4$, known from the early seminal work of Sommerfeld. This experimental fact should be compared with the prediction of the LS rule (2.19).

$\eta = m_N c^2/U$ is now negative and, with $m_N c^2 = 0.5$ MeV and $U(r_0) = -2.72 \times 10^{-5}$ MeV for the hydrogen atom and the Bohr's radius r_0, it follows that, in the atomic case, the characteristic value is $\eta \approx -2 \times 10^4$. For large absolute values of η, the expression Eq. (2.19) reduces to x $\sim \mid \eta \mid \sim 1/\alpha_{EM}^2 \approx 10^4$, in agreement with the empirical value quoted above. The fine structure of atomic spectra thus becomes a limit of the spin-orbit rule (2.19). It should be stressed again the validity of the spin-orbit rule in Coulomb-like systems is due to the 1/r behavior of the potential.

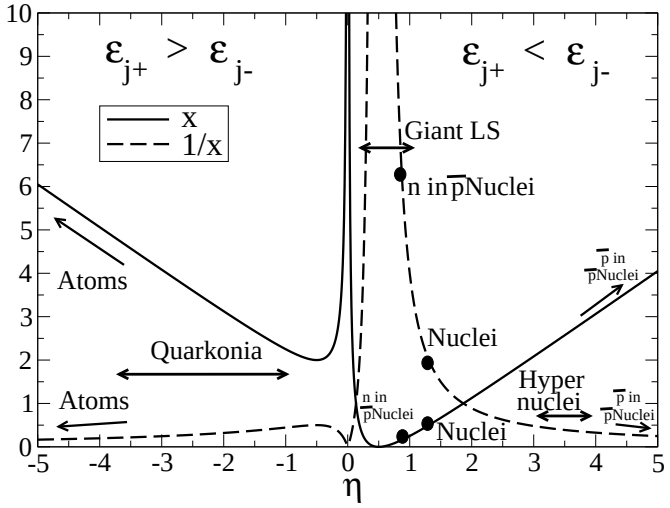

Figure 2.4: The ratio between the principal energy spacings and the spin-orbit splittings (fine structure) Eq. (2.19), as a function of the ratio η (Eq. 2.20) between the mass of the particle and the effective potential that determines the spin-orbit force in a given quantum system.

Figure 2.4 displays the LS rule, which is a generalisation of the fine structure constant in order to evaluate the spin-orbit effect in various systems. It should be noted that a giant LS state is predicted for η=1/2, where the LS gap becomes larger than the HO one.

The particular dependence of the x ratio on η, shown in Fig. 2.4, also allows to predict the sign of V_{LS}. For positive values of η, states for which the orbital angular momentum and spin are aligned are found at lower energy with respect to states for which the orbital angular momentum and spin are anti-aligned (nuclei, hypernuclei), whereas the opposite energy ordering is found for negative η (atoms, quarkonia). The ratio x (Eq. (2.19)) diverges at $\eta = 0$, that is, in the limit of massless particle where no spin-orbit effect is possible in this framework.

Chapter 3

The case of nuclei

The nucleus is a manybody system in which nucleons potentially interact through all the four interactions provided by the Nature. This is a quite unique manybody system. As discussed in Chapter 1, the strong interaction dominates over all the other interactions, including the electromagnetic one. It is therefore a good approximation to only consider, as a first step, the strong interaction among nucleons to describe nuclear structure. Another specificity of nuclei is that the constituents are of two different types: neutrons and protons. This is also rather rare in manybody systems were only one type of constituent is usually involved. Finally the last specificity of nuclei is that nucleons are non-elementary particles. Any nucleonic interaction should take this effect into account at least in an effective way.

3.1 The nucleon-nucleon interaction

The nucleon-nucleon interaction is considered as an effective expression of the QCD interaction among quarks and gluons of the nucleons. In this approach, the nucleon-nucleon interaction can be approximated by meson exchanges, as depicted on Figure 3.1, taken from effective field theory. It should be noted that a 3-nucleons interaction appears at the third order. This is how effective interactions takes into account the non-elementary structure of nucleons: two nucleons gets polarised in the presence of a third one, generating a specific 3-body interaction. More generally one should expect that the nucleon-nucleon interaction depends on the nucleonic density of the nucleus.

In a more phenomenological way, the nucleon-nucleon interaction (labelled V' in Eq. 2.1) can be described with various mesons exchanges as depicted on Figure 3.2.

Formally, the meson exchange potential corresponds to a generalisation of a Coulomb-like potential to massive mediators. In the vacuum, the photon propagation is described by a potential Φ, following the Maxwell equation

$$\Box\Phi(\vec{r},t) = 0 \tag{3.1}$$

In the statical case, Eq. (3.1) provides a $\Phi \sim$1/r potential. In order to generalise this approach to massive mediators, one should use the quantum mechanics correspondence principle: Eq. (3.1)

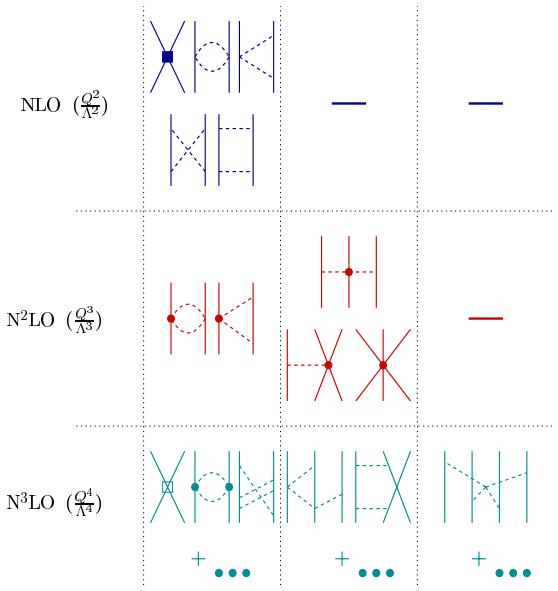

Figure 3.1: Hierarchy of the nuclear interactions obtained with effective field theory. Lines are nucleon propagators and dashed lines are mesons one. From arXiv:nucl-th/0409028.

can be derived from the momentum/energy relation of the photon (E^2=p^2c^2) with the following relations:

$$E \rightarrow i\hbar\frac{\partial}{\partial t} \qquad and \qquad \vec{p} \rightarrow -i\hbar\vec{\nabla} \tag{3.2}$$

Eq. (3.1) is therefore rederived since

$$\Box = \Delta - \frac{1}{c^2}\frac{\partial^2}{\partial t^2} \tag{3.3}$$

In order to generalise the above demonstration to a massive mediator with mass m_0 >0, the momentum/energy relation of a massive particle is

$$E^2 = p^2c^2 + m_0^2c^4 \tag{3.4}$$

Using the (3.2) relations, Eq. (3.4) becomes

$$(\Box - \mu^2)\Phi(\vec{r}, t) = 0 \tag{3.5}$$

with

$$\mu \equiv \frac{m_0 c}{\hbar} \tag{3.6}$$

Eq. (3.5) is the Klein-Gordon equation which drives the propagation of a free particle in the vacuum. Its solutions provides the potential corresponding to massive mediators. In the stationary and spherical symmetric case, Eq. (3.5) becomes

$$\frac{d^2(r\Phi)}{dr^2} = \mu^2.(r\Phi) \tag{3.7}$$

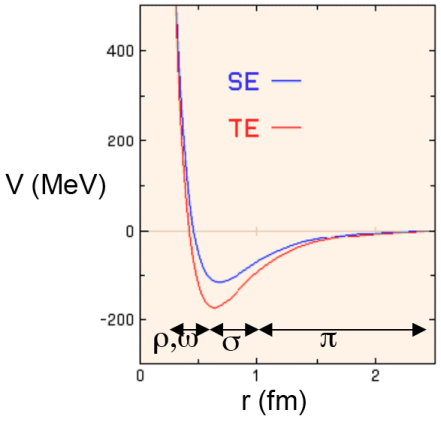

Figure 3.2: The nucleon-nucleon interaction generated by mesons exchanges

which solution is

$$\Phi(r) = g\frac{e^{-\mu r}}{r} \tag{3.8}$$

This is the so-called Yukawa potential, displayed on Fig. 3.3. The range r_0 (see Chapter 1) of this potential is

$$r_0 = \mu^{-1} = \frac{\hbar}{m_0 c} \tag{3.9}$$

Therefore r_0 and m_0 carry the same information.

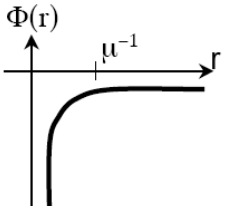

Figure 3.3: The Yukawa potential (Eq. (3.8) with $g < 0$)

The typical range of the nucleon-nucleon interaction ($r_0 \sim$ 1,5 fm, see Chapter 1) implies through Eq. (3.9) a mesonic mediator of $m_0 \simeq 140$ MeV. This corresponds to the pions, which are the lightest mesons. At shorter range the attractive part of the nucleon-nucleon interaction is therefore described by a Yukawa potential with a heavier meson (the σ). Finally at very short range, the hard repulsive core of the interaction is described by the exchange of heavier mesons (the ω and the ρ of masses about 800 MeV). Therefore the nucleon-nucleon interaction V' (Fig. 3.2) can be described by a superposition of Yukawa potentials (3.8) from 2 attractive (π, σ) an 2 repulsive (ω, ρ) mesons. It should be noted that the attraction is rooted in the J=0 (scalar) total

angular momentum of the π and σ and the repulsion in the J=1 (vector) total angular momentum of the ω and the ρ.

Fig. 3.2 shows that the nucleon-nucleon interaction is attractive with a large repulsive hard core. Therefore, the density of nucleons is expected to saturate in the center of the nucleus: if the number of nucleons increases, the size of the nucleus will increase because of the hard core, but not its density. This is well illustrated on Fig. 3.4 where the charge (proton) density of light to heavy nuclei has been measured: the bulk density remains similar among nuclei. The volume of the nucleus being proportional to the number A of nucleons, as a first approximation, its radius R will be proportional to $A^{1/3}$: R=$r_0 A^{1/3}$.

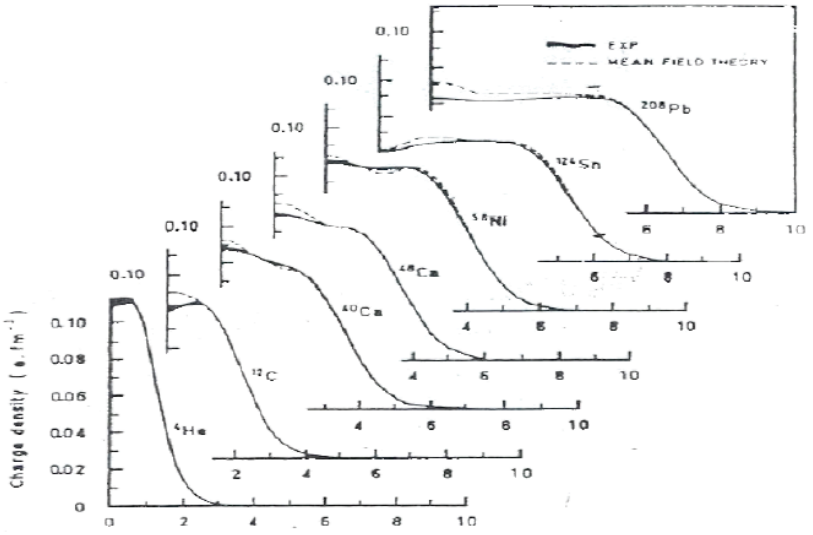

Figure 3.4: Measured (by electron scattering) and calculated charge density in ^{4}He, ^{12}C, ^{40}Ca, ^{48}Ca, ^{58}Ni, ^{124}Sn and ^{208}Pb nuclei.

3.2 Mean-field and spin-orbit potentials

As discussed in section 2.1, for QL systems such as nuclei, it is a good approximation to consider the mean potential V(r) felt by each nucleon, built from the nucleon-nucleon interaction V'. Eq. (2.12) show that the confining potential V(r) is generated by the sum of the vector U(r) and scalar S(r) potentials, which are themselves generated by the mesons fields discussed above. For instance in an approximation where the S(r) attractive part of the nucleon-nucleon interaction is generated by the σ meson and the U(r) repulsive part by the ω and ρ, one gets the confining potential in nuclei displayed on Figure 3.5.

The shapes of the potential can be deduced from the short range of the nucleon-nucleon interaction, compared to the size of the nucleus and the delocalisation of the nucleons. Approximating V' by a Dirac delta function $\delta(\vec{r}-\vec{r'})$ in Eq. (2.1) yields the same spatial behavior for the mean po-

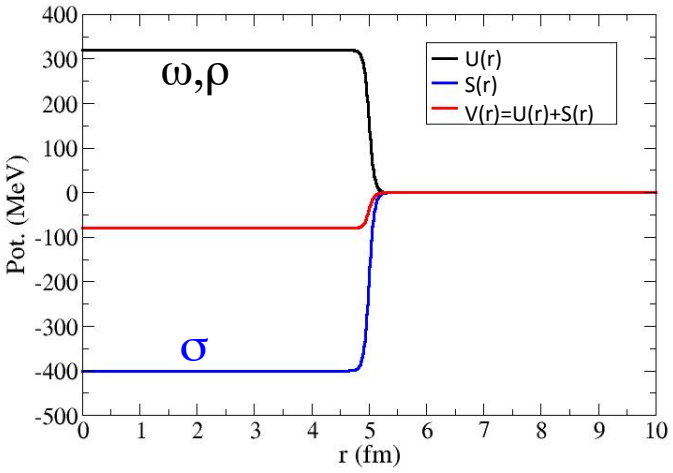

Figure 3.5: The mean vector (U), scalar (S) and total (V) potentials at work in nuclei

tential V and the density of the nuclei ρ. Since the nuclear density has a typical constant behavior (Fig. 3.4), so do the mean potentials (Fig. 3.5).

The vector potential U (short-range repulsion) has a typical strength of ≈ 350 MeV, and the scalar potential S (medium-range attraction) is typically of the order of -400 MeV in nucleonic matter and finite nuclei. Although of large magnitude, these two potentials mostly cancel and the final confining nuclear potential is V=U+S$\simeq$-70 MeV.

In the case of the nuclear spin-orbit potential, it originates from the difference between the two large fields U and S as shown by Eq. (2.13). Figure 3.6 shows that $U - S \approx 750$ MeV. As discussed in section 2.2, the impact of the spin-orbit on the nuclear shell structure is important and this is due to the close value of the nucleon mass ($m_N c^2 \simeq$940 MeV) and the $U - S$ value: the largest spin-orbit splittings are comparable in magnitude to the energy gaps between major shells of the nuclear potential.

3.3 The shell structure

As discussed in section 2.2, the nucleonic states will therefore be structured around HO states, with strong degeneracy raising due to the important spin-orbit effect in nuclei. Indeed Fig. 2.4 shows that the energy shell gap arising from the spin-orbit is of the same order of magnitude than the natural HO discretisation one. A typical nucleonic energy sequence is displayed on Fig. 3.7

It shows that the major energy gaps are first driven by the HO discretisation (magic numbers 2,8 and 20) and then driven by the spin-orbit effect (from 28 and above), as it can be understood from Eq. (2.18): the spin-orbit gap increases with the orbital quantum number ℓ.

Fig. 3.7 also shows a prior degeneracy raising with respect to the angular momentum of the

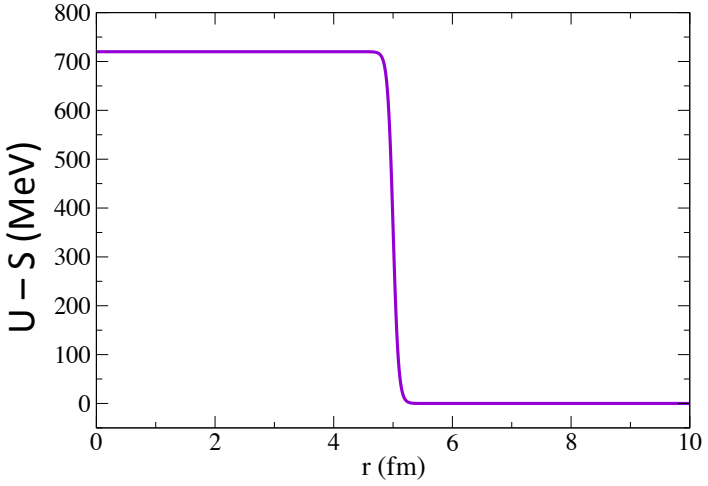

Figure 3.6: The mean vector (U) minus the scalar (S) at work in the spin-orbit potential (Eq. (2.13))

HO states. This is due to the fact that the HO potential does not well describe the diffuseness on the surface of the nucleus (compare the diffuseness of Figs 3.4, 3.5 and 2.2). Hence it is convenient to add to the central part of the potential a term which takes into account this diffuseness, namely :

$$V(r) = V_{OH}(r) - D\hat{\ell}^2 \tag{3.10}$$

where D is a constant. The nucleonic wavefunctions at the surface of the nucleus are more impacted by this additional term because they involve the largest ℓ values of the system. The energetical effect of this term is to raise the degeneracy by a -D$\hbar^2\ell(\ell+1)$ value.

It should be noted that the nuclear central term (3.10) is well described by a direct analytical potential, the so-called Woods-Saxon potential:

$$V(r) = \frac{-V_0}{1 + e^{\frac{r-R}{0.228a}}} \tag{3.11}$$

where a is the diffusivity of the potential. Fig 3.8 displays a comparison of the HO and the Woods-Saxon potential, showing a more accurate behavior of the last one to describe both the nuclear saturation and the correct diffuseness of the confining potential.

Finally one should remind that Fig. 3.7 only provides a typical and simple solution of the nuclear many body problem. The best up-to-date solution makes the full use of the Dirac equation (2.8) for each nucleus, allowing for deformation effects and using the best possible nucleon-nucleon interaction, possibly derived from QCD-related effective field theory.

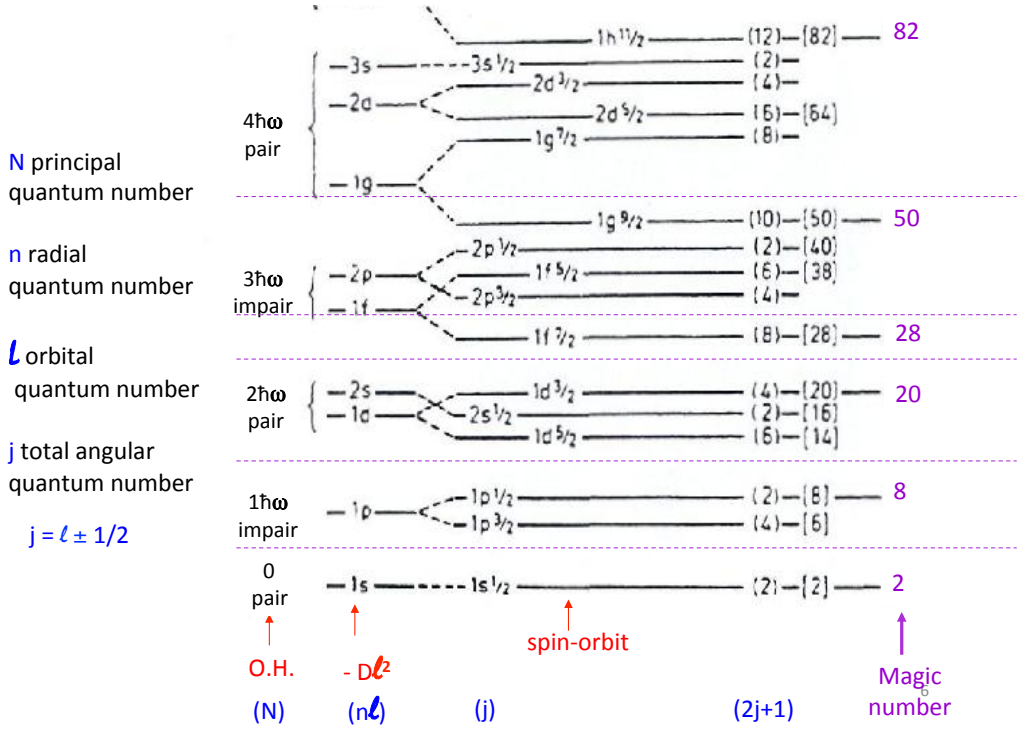

Figure 3.7: The typical shell structure of nucleonic state in nuclei

3.4 The isospin symmetry

The strong interaction obeys to the isospin symmetry, based on the close degeneracy of the up and down quark masses. This is described by the SU(2) group, in total analogy with the spin 1/2 degeneracy case: there are 3 isospin Pauli matrices, etc. The only difference is that the isospin space is different from the spatial space whereas the spin symmetry occurs in the spatial space.

The proton and neutrons being built from u and d valence quarks, it is understandable that they should also obey to an SU(2) isospin symmetry at their level. Indeed the neutron and proton masses are very close, 939.5 MeV and 938.2 MeV, respectively. This little mass difference is due to the Coulomb interaction which impacts the proton and not the neutron, but also to the small SU(2) isospin breaking: the u and d quarks have not exactly the same masses.

Proton and neutron belong to a t=1/2 doublet, where t is the isospin quantum number, and with t_3=1/2 for the proton and t_3=-1/2 for the neutron. t_3 is the projection of the isospin on the third axis of the isospace.

Let us consider a 2 nucleons system, which encompasses the simplest nucleus: the deuteron. The total isospin T of this system is therefore T=0 or T=1 due to the analogy with the coupling of two 1/2 angular momentum in quantum mechanics. The Clebsch-Gordan coupling provides :

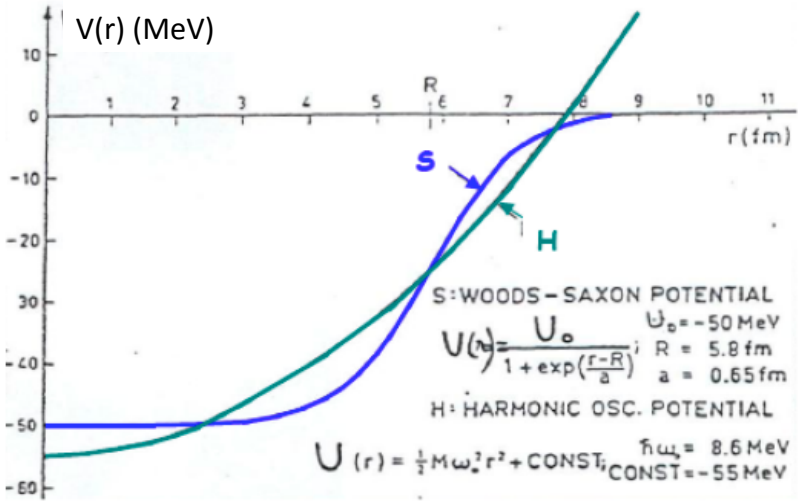

Figure 3.8: Comparison between the HO (labelled H) and Woods-Saxon (labelled S) confining potentials.

$$\begin{cases} |1\ 1\rangle = |p\ p\rangle \\ |1\ 0\rangle = \frac{1}{\sqrt{2}}(|p\ n\rangle + |n\ p\rangle) \\ |1\ -1\rangle = |n\ n\rangle \end{cases} \quad \text{Triplet state}$$

$$|0\ 0\rangle = \frac{1}{\sqrt{2}}(|p\ n\rangle - |n\ p\rangle) \quad \text{Singlet state}$$

The triplet state is symmetric with respect to the exchange of the two nucleons whereas the singlet state is anti-symmetric. Since the total wavefunction of a fermionic system has to be anti-symmetric with respect to the exchange of two fermions, L+S+T should be odd. L is the total angular momentum of the 2 nucleons system and S is its total spin. It should be reminded that for identical fermion L+S has to be even, to be anti-symmetric under the exchange. The L+S+T condition is a generalisation to a system of non-identical fermions, namely a system of protons and neutrons.

Moreover the nucleon-nucleon interaction can bound a system of 2 nucleons only if they are in the L=0 and S=1 state. Therefore the generalised Pauli principle imposes T=0 which is the singlet state: only a np (deuteron) system is bound, and not the nn nor the pp one.

It should be noted that the interaction among two nucleons allows for pairing. This generates superfluidity at the nucleus' scale. This is the Cooper mechanism, in which superfluidity can arise when a short range and attractive interaction acts among fermions. The two nucleons gets paired in a L=0 total angular momentum where the pairing interaction is the most intense. There are therefore two possibilities: T=1 and S=0 which corresponds to pairing among identical nucleons

with spin anti-aligned, but also a specific nuclear channel: T=0 and S= 1. In this last case a neutron and a proton can get paired with spin aligned. This is a very specific channel at work in nuclei, and several corresponding experimental signals have been recently obtained.

The isospin formalism is identical to the spin one. In the case of a system invariant by rotation in the isospace (where its axis are labelled 1, 2 and 3), the isospin of the system is conserved by the strong interaction:

$$\left[\hat{H}_F, \hat{T}\right] = 0 \tag{3.12}$$

In practice this allows the stationary wavefunctions of the system to be labelled by the quantum numbers which are the eigenvalues of T^2 (the Casimir operator) and T_3: they both commute among them and also with H. The isospin part of the wavefunction $\mid TT_3 >$ reads

$$\hat{T}^2 \mid T, T_3 >= T(T+1) \mid T, T_3 > \tag{3.13}$$

$$\hat{T}_3 \mid T, T_3 >= T_3 \mid T, T_3 > \tag{3.14}$$

In the case of a single nucleon (t=1/2), its isospin is described by the Pauli matrices (generators of SU(2)):

$$\hat{t}_i = \frac{1}{2}\tau_i \tag{3.15}$$

with

$$\tau_1 = \begin{pmatrix} 0 & 1 \\ 1 & 0 \end{pmatrix} \qquad \tau_2 = \begin{pmatrix} 0 & -i \\ i & 0 \end{pmatrix} \qquad \tau_3 = \begin{pmatrix} 1 & 0 \\ 0 & -1 \end{pmatrix} \qquad \tau_{1,2,3}^2 = \begin{pmatrix} 1 & 0 \\ 0 & 1 \end{pmatrix} \tag{3.16}$$

The Pauli matrices obey to the commutation relations:

$$[\tau_i, \tau_j] = 2i\tau_k \tag{3.17}$$

$$\left[\tau^2, \tau_i\right] = 0 \tag{3.18}$$

The isospin creation and annihilation operators

$$\hat{t}_\pm = \hat{t}_1 \pm i\hat{t}_2 \tag{3.19}$$

are described by

$$\hat{t}_+ = \begin{pmatrix} 0 & 1 \\ 0 & 0 \end{pmatrix} \qquad \hat{t}_- = \begin{pmatrix} 0 & 0 \\ 1 & 0 \end{pmatrix} \tag{3.20}$$

They allow to increase or decrease the t_3 value:

$$\hat{t}_+ \mid p >= 0 = \hat{t}_- \mid n > \qquad \hat{t}_+ \mid n >=\mid p > \qquad \hat{t}_- \mid p >=\mid n > \tag{3.21}$$

The isospin symmetry implies that the mean potentials for neutron and proton in a nucleus are very similar. Figure 3.9 displays such potentials. The shell structure is the dominant pattern.

The main difference between the neutron and proton potentials is that protons feels the Coulomb one in addition to the strong potential. The last nucleonic level occupied by protons (neutrons) is called the proton (neutron) Fermi level.

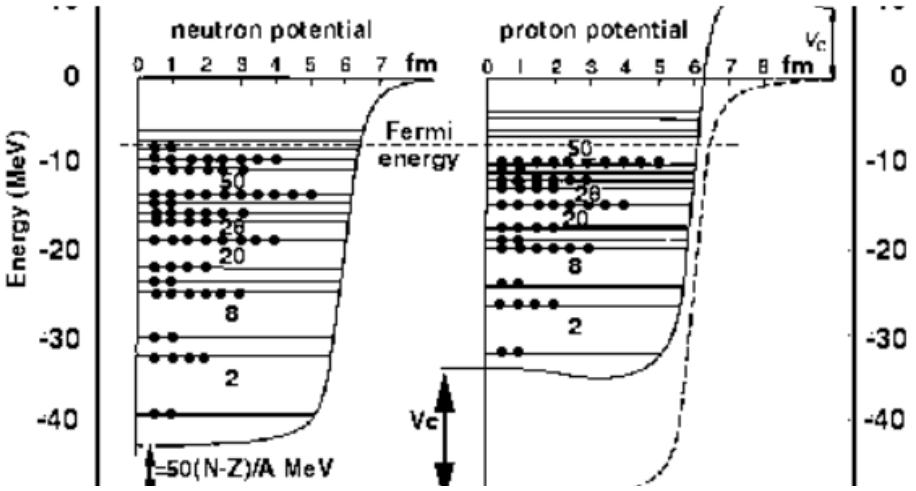

Figure 3.9: The mean neutron and proton confining potentials in the ^{116}Sn nucleus.

3.5 The nuclear chart

The results above provide the main methods to describe and predict the nuclear structure. The phenomenology to be understood is varied and involves binding limits by the strong interaction (driplines), a large variety of nuclear states (QL, clusters, haloes, deformations, etc.), numerous radioactivities based on 3 of the 4 fundamental interactions of Nature. Moreover nuclei are involved in astrophysical processes. Figure 3.10 sketches a few examples of nuclear phenomena to be described in an unified framework.

Based on current nuclear structure predictions, it is believed that there exists about 7000 bound nuclei. Only 300 (5%) of them are stable. The majority of unstable nuclei have not been produced yet on frontline Earth-based facilities such as the Riken (Japan) or the ISOLDE (Cern) ones.

It is the aim of the next chapters to understand these phenomena (Fig. 3.10) in an unified way.

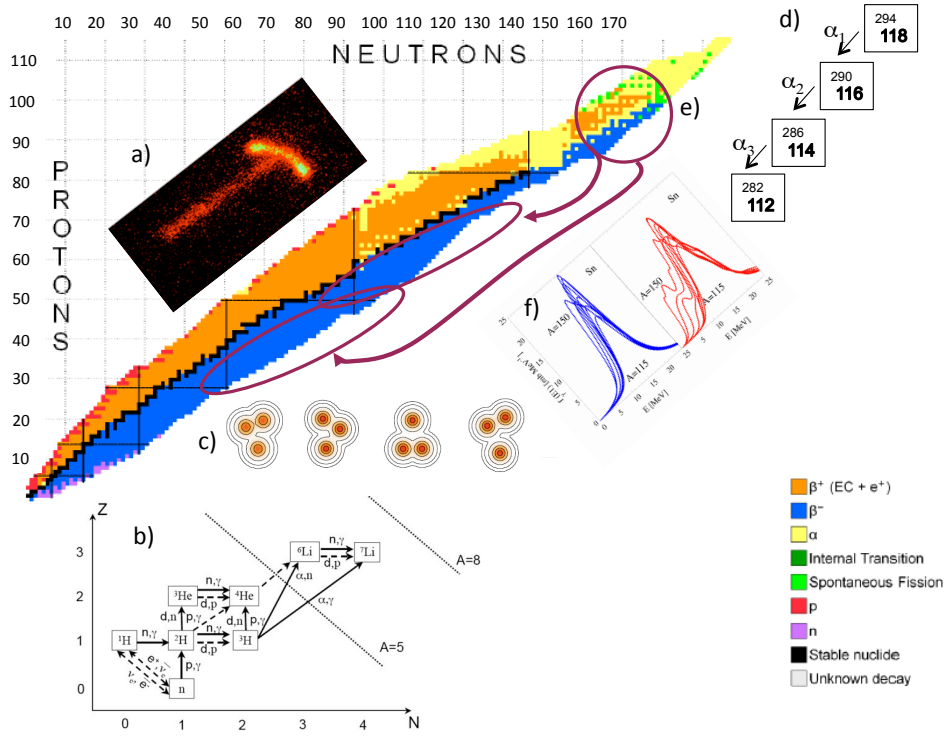

Figure 3.10: The nuclear chart and phenomenology: a) 2 protons radioactivity, b) light elements nucleosynthesis, c) clusterisation, d) superheavy nuclei, e) fission and f) exotic modes of excitations.

Chapter 4

Nuclear states

A relevant way to describe in an unified way the main various nuclear states is to consider their localisation properties.

4.1 Localisation

The localisation property of the system is indeed driven by the λ_N/r_0 ratio where λ_N is the constituent wavelength (Fig. 2.1). Quantum effects start to have an impact from the solid to the quantum liquid states. This happens when the typical dispersion of the constituents is non-negligible compared to the inter-constituents distance. When λ_N is larger than the typical interconstituent distance r_0, the system reaches a QL state. The inverse case corresponds to a crystal state where the constituents are confined at the nodes of the crystal (see Fig. 1.1).

It can be demonstrated that, using Eqs. (1.6):

$$\frac{\lambda_N}{r_0} \simeq \pi\sqrt{2}\sqrt{\Lambda} \tag{4.1}$$

which shows that the quantality drives the localisation property of the system. Using (1.7), Eq. (4.1) becomes

$$\frac{\lambda_N}{r_0} = \frac{\pi\sqrt{2}}{\mathcal{A}} \simeq \frac{5}{\mathcal{A}} \tag{4.2}$$

It should be noted that the wavelength of a constituent can be approximated by

$$\lambda_N = \frac{h}{p_N} \simeq \frac{\hbar}{\sqrt{2mkT}} \tag{4.3}$$

where the kinetic energy of the constituent is approximated by kT. Decreasing temperature (or increasing density) generates a larger dispersion of the wavefunction of the constituent, which can lead to quantum effects when λ_N is non-negligible compared to the inter-constituents distance r_0. This means that in a dense system (quantum liquid) the filling of the space between the nodes of the crystal is done so to achieve a homogeneous density but with the quantum side-effect that the constituents get also delocalised. The λ/r_0 ratio (4.1) is therefore relevant to analyse these delocalisation effects. However this ratio does not take into account any finite size effect: it is

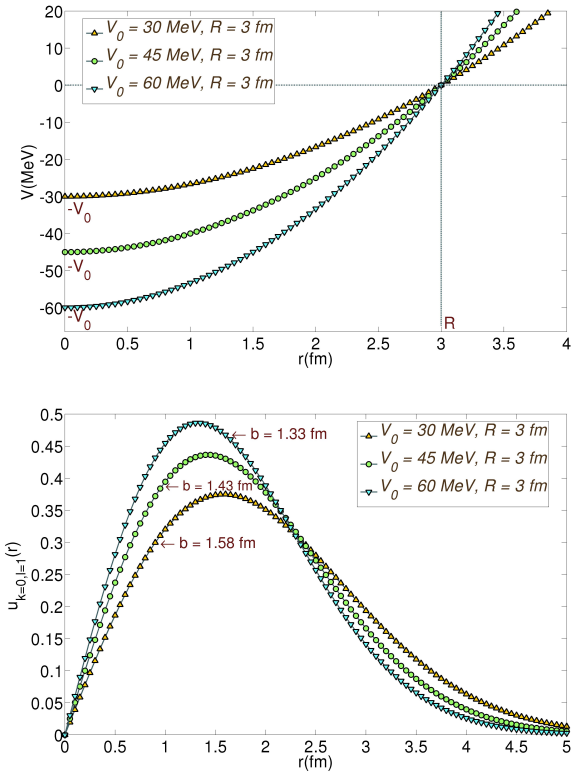

Figure 4.1: Top: Harmonic oscillator potentials for three different values of the depth: V_0=30, 45 and 60 MeV, with the same radius R = 3 fm. Bottom: the radial wave functions of the corresponding first p-state. The position of the maximum is determined by the oscillator length b.

the same whether the system has a few constituents or an infinite number. A more accurate ratio should be used in finite systems such as nuclei, where surface effects are not negligible.

In finite systems, a relevant quantity is the b/r_0 ratio where b is the typical dispersion of a constituent taking into account the finite size of the system. Fig. 4.1 shows the evolution of the spreading b of a nucleon wavefunction in a confining potential with various depths.

Approximating the confining nuclear potential by an HO one, it is possible to derive an analytical expression for b, which is approximated by the harmonic oscillator length. The localisation parameter is therefore defined as

$$\alpha_{loc} \equiv \frac{b}{r_0} = \frac{\sqrt{\hbar} A^{1/6}}{(2 m_N V_0 r_0^2)^{1/4}} \tag{4.4}$$

where A is the number of constituent of the system and V_0 (>0) the depth of the confining potential.

Eq. (4.4) allows to study the evolution of the states with respect to the number of constituents A and is well adapted to systems where finite-size effects are relevant ($A \lesssim 10^3$) such as nuclei. It should be noted that α_{loc} should not be mixed with a coupling constant as defined in Chapter 1, also labelled by the α Greek letter.

4.2 Nuclear states

Fig. 4.2 displays various nuclear states. They can be ordered along the α_{loc} value. Haloes nuclear states are the most delocalised one. When the localisation parameter decreases the quantum liquid nuclear state is the most frequent to be found in Nature. It exhibits an homogeneous density due to the large delocalisation of the nucleons wavefunctions. When the localisation parameter further decreases, the inter-nucleon spreading starts to be of the order of the inter-nucleon distance. In this optimal overlap, the system reaches an hybrid state between the QL and the crystal: nucleons arrange in clusters, a kind of nuclear molecules, where the density is non-homogeneous. Finally when the localisation parameter is much smaller than 1, the nuclear crystal state is reached.

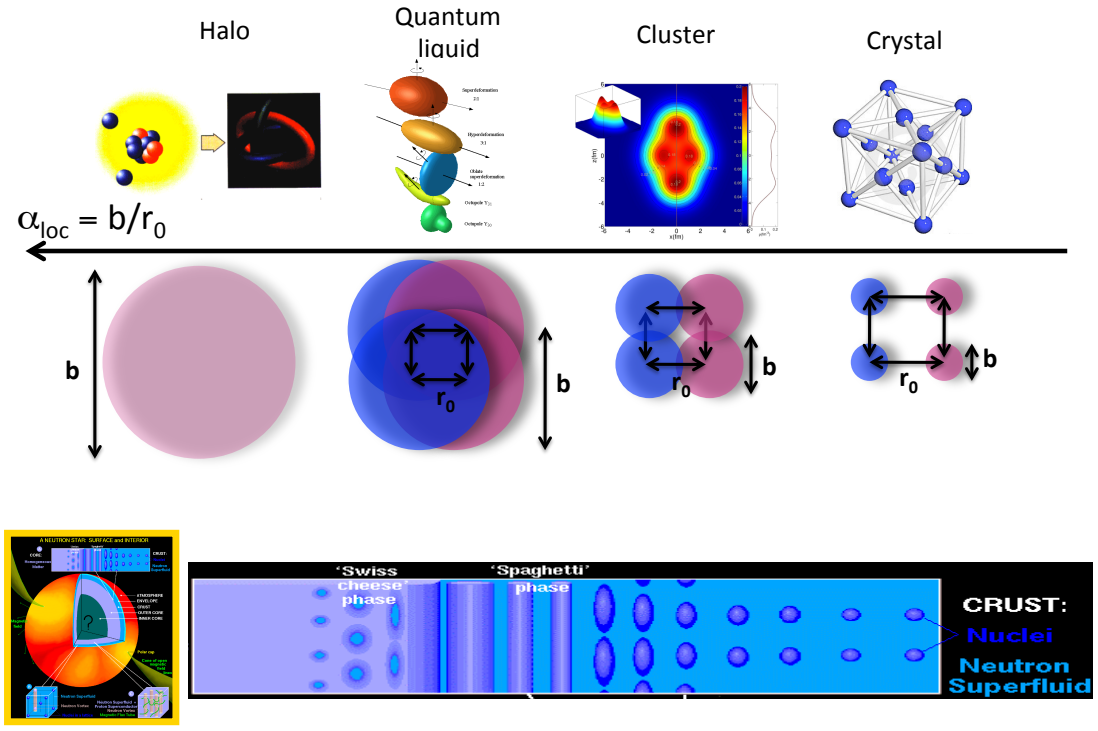

Figure 4.2: The various nuclear states ordered with the localisation parameter α_{loc} (Eq. 4.4). Bottom: the predicted structure of the inner crust of a neutron star (bottom left).

Haloes, QL, and cluster states have been experimentally evidenced. The localisation parameter allows to grasp the various nuclear states in an unified way. But why has the nuclear crystal state not been discovered so far ?

Figure 4.3 displays the evolution of α_{loc} with A, for a typical value of V_0= 70 MeV. The localization parameter α_{loc} generally increases with the number of nucleons (see Eq. 4.4) and, therefore, cluster states are more easily formed in light nuclei, as observed experimentally. The

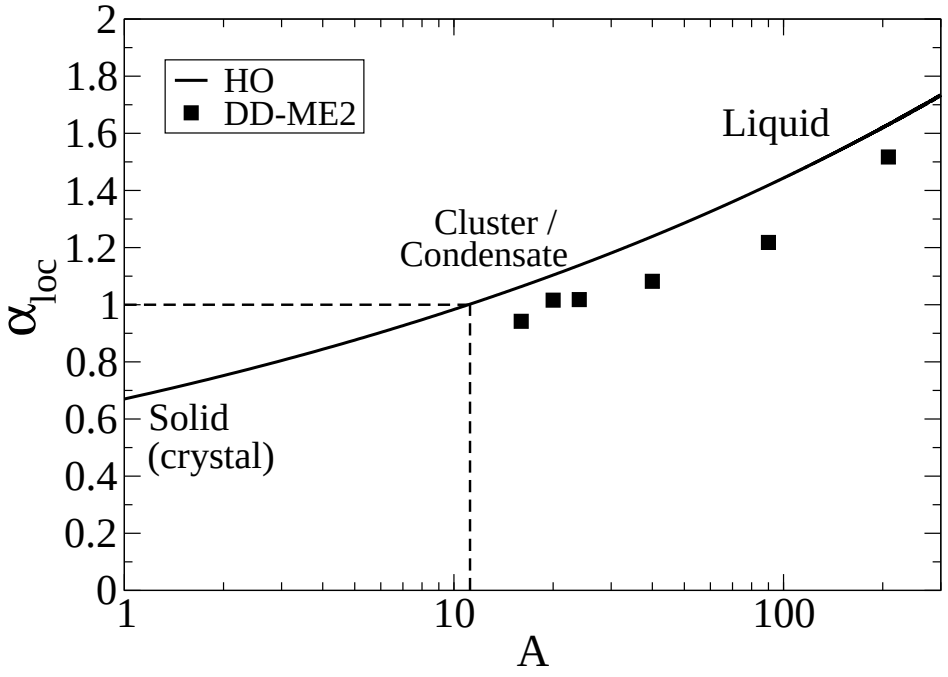

Figure 4.3: The localization parameter α_{loc} (Eq. (4.4)) as a function of the number of nucleons. The average values of α_{loc} for ^{16}O ^{20}Ne, ^{24}Mg, ^{40}Ca, ^{90}Zr, calculated for the microscopic self-consistent solutions obtained using the Dirac equation, are denoted by squares.

transition from localized clusters to a liquid state ($\alpha_{loc} \sim 1$) occurs for nuclei with $A \approx 30$. For heavier systems α_{loc} is considerably larger than 1 and, therefore, heavy nuclei consist of largely delocalized nucleons and this explain their liquid drop nature and the large mean free path of nucleons. More precisely, nuclei are in the Fermi liquid phase and localized cluster states (hybrid phase) can be formed in light nuclei. Fig. 4.3 also illustrates the fact that a crystal phase ($\alpha_{loc} \lesssim 0.8$) cannot occur in finite nuclei: the number of corresponding nucleons becomes too small. However, Nature may offer the possibility of existence of nucleonic crystals in the crust of neutron stars (Fig. 4.2), where crystallization is caused by the long range Coulomb interaction in a gravitationally constrained environment. The transition between the crystal and the quantum liquid in the neutron star crust can be described by various models: gelification, Coulombic frustration or quantum melting. The crystal case in the crust of neutron star is based on a different effect than in nuclei: the frustration effect comes from the Coulomb Wigner crystal imposed by the gravitational constraints. This is not the case in nuclei. It is therefore unexpected that a nuclear crystal state can occur in nuclei: clusters states are the most visible hybrid states close to the crystal one, which can be reached in a nucleus.

In the case of nuclei, saturation plays a key role in the emergence of clusters. In a saturated system there is a natural length scale - the equilibrium inter-particle distance due to the interaction,

which in nuclei is $r_0 \simeq 1.2$ fm. Because of this characteristic length scale, nucleons tend to form clusters when the spatial dispersion of the single-particle wave function is of the order of r_0. Eq. (4.4) allows to show that in a large nucleus the localization parameter α_{loc} increases since V_0 remains rather constant due to saturation. Because of the approximate $A^{1/6}$ dependence of α_{loc}, medium-heavy and heavy nuclei will exhibit a quantum liquid behavior, whereas cluster states can occur in light nuclei.

4.3 The deep relativistic confining potential

Eq. (4.4) shows that the depth of the confining potential also plays a crucial role in the localisation properties of the constituents. It is not possible to change the depth of potential experimentally, but this can be done theoretically, by using various nucleon-nucleon interactions V' which predict different depth V_0 of the potential. It is especially the case between interactions derived for the Dirac equation in nuclei (relativistic ones) and interactions derived for the Schrödinger equation in nuclei (non-relativistic ones). As explained in section 2.2 the depth of a relativistic potential is determined by the difference of two large fields: an attractive (negative) Lorentz scalar potential of magnitude 400 MeV, and a repulsive Lorentz vector potential of magnitude 320 MeV (plus the repulsive Coulomb potential for protons). The choice of these potentials is further constrained by the fact that their sum ($\sim$ 700 MeV) determines the effective single-nucleon spin-orbit potential. In a non-relativistic approach the spin-orbit potential is included in a purely phenomenological way, with the strength of the interaction adjusted to empirical energy spacings between spin-orbit partner states. Since the relativistic scalar and vector fields determine both the effective spin-orbit potential and the self-consistent single-nucleon mean-field, for all relativistic functionals the latter is found to be deeper than the non-relativistic mean-field potentials, for which no such constraint arises. Fig. 4.3 displays both relativistic and non-relativistic single-neutron potentials in the ^{20}Ne nucleus: the relativistic one is deeper.

The deeper the potential, the smaller the oscillator length, and the wave functions become more localised (see Eq. (4.4)). At the origin of nuclear clustering is, therefore, the depth of the self-consistent single-nucleon mean-field potential associated with the nucleon-nucleon interaction. It should be noted that the depth of the potential is not an observable, which can explain that different approaches predict different depths. However the relativistic one is more sound for the reason explained above. Figure 4.3 shows the predicted density in ^{20}Ne in both approaches. ^{20}Ne is experimentally known to exhibit clusterisation signals; this is the case of the relativistic density where high density clusters are predicted.

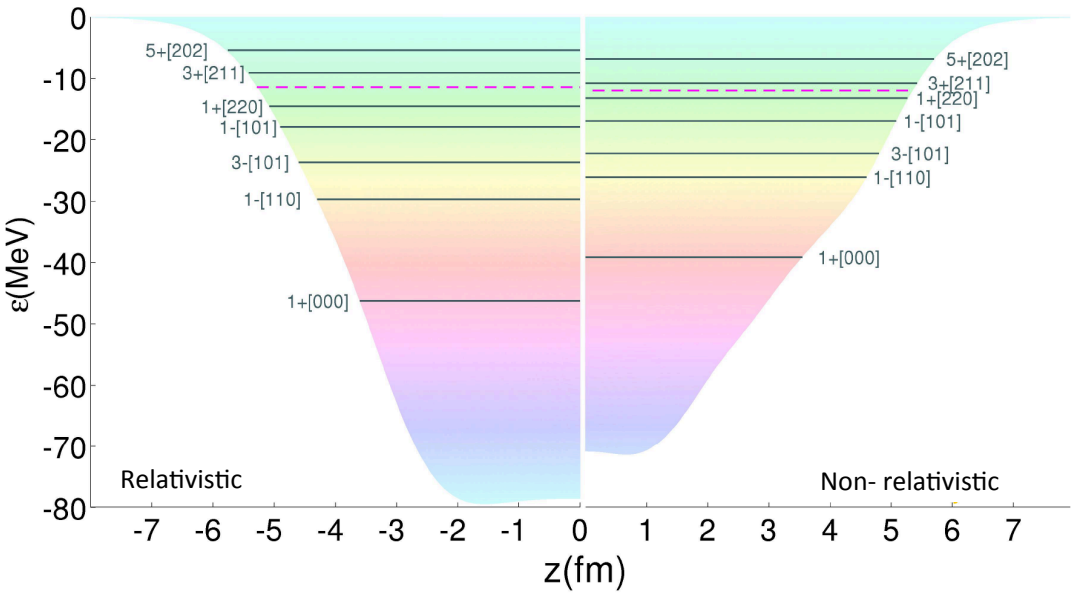

Figure 4.4: The relativistic (left) and non-relativistic (right) confining potentials predicted in the ^{20}Ne nucleus

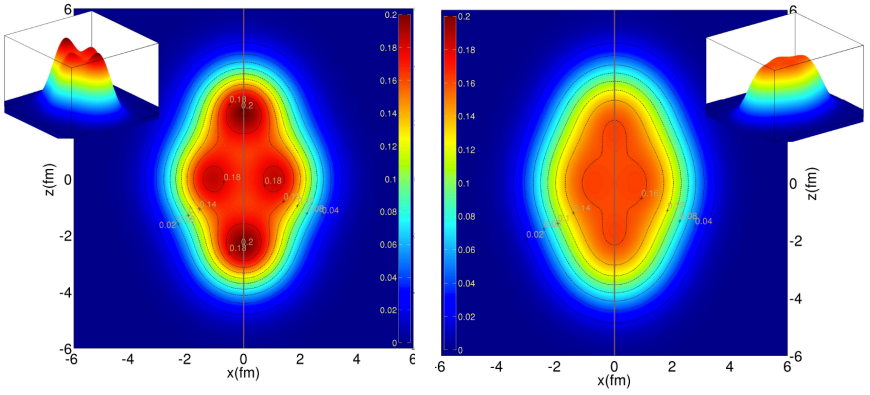

Figure 4.5: The nucleonic density in ^{20}Ne predicted with relativistic (left) and non-relativistic (right) approaches.

Chapter 5

Radioactivities

Both radioactivities and nuclear reactions are described by the transformation of an initial nuclear state Ψ_i into a final one Ψ_f through the use of one of the 3 (strong, electromagnetic or weak) interaction V_{int}. The key quantity to be calculated is

$$< \Psi_f \mid \hat{V}_{int} \mid \Psi_i > \tag{5.1}$$

It allows to predict the mean-lifetime in the case of a radioactive decay (present chapter) or the cross section (Chapter 6) in the case of a reaction. In the first case the transition from the initial state towards the final one is spontaneous (Q-value >0) whereas energy has to be provided in the latter case (Q<0). The Q-value is defined as

$$Q = \sum_i m_i c^2 - \sum_f m_f c^2 \tag{5.2}$$

where, in a radioactive decay, i is the mother nucleus whereas f runs over the daughter nucleus and the possible emitted particles in the decay process.

5.1 A dozen radioactivities

A radioactive decay corresponds to the emission of a particle by the mother nucleus. Nuclear stability is defined as the absence of any radioactivity. It should be noted that the determination of the nuclear stability is in principle impossible to prove experimentally. For instance, ^{209}Bi was considered as a stable nucleus, but in 2003 high precision decay measurements showed that it is indeed an α emitter with a mean-lifetime of 10^{19} years.

If the Hamiltonian h responsible for the radioactive decay is a perturbation compared to the total Hamiltonian H of the system, the transition probability λ of the radioactive decay can be calculated using the Fermi golden rule:

$$\lambda = \frac{2\pi}{\hbar} \mid< f \mid \hat{h} \mid i >\mid^2 \xi(E) \tag{5.3}$$

where ξ(E) is the density of final states.

This is the case for radioactive decay induced by the electromagnetic or the weak interactions which are small compared to the strong interaction generating the nuclear structure. In the case of radioactive decays by the strong interaction, Eq. (5.3) cannot be used, and the full time dependent Dirac or Schrödinger equation should be used instead. This is close from a nuclear reaction description and in practice several approximations are used.

It should be noted that radioactive decays were one of the first quantum mechanical process which have been directly observed, before setting up the quantum mechanics theory. The surprising (at that time) random character empirically extracted from the measured decay laws is nothing but the transition probability (5.1).

The various radioactive decays are indeed much richer than the first 3 letters of the Greek alphabet. Each interaction generates its own radioactive decay and it is much more relevant to order such decays as a function of the interaction rather than Greek letters. Table 5.1 summarizes radioactive decays known today. The two striking features are i) they are more than a dozen and ii) such decays have been recently discovered. Indeed several additional decay modes are predicted and may be discovered in the forthcoming years.

Interaction	**Radioactivity (Date of discovery)**	**Particles emitted by the mother nucleus**
Electromagnetic	γ (1900)	photon
	Internal conversion (1938)	e^-
	2γ (1987)	2 photons
	2γ vs.γ (2015)	2 photons
Weak	β^- (1898)	e^-, $\bar{\nu}_e$
	β^+ (1933)	e^+, ν_e
	Electronic capture (1937)	ν_e
	Double β^- (1980)	$2e^-$, $2\bar{\nu}_e$
	Double electronic capture (2001)	$2\nu_e$
	Bound state β^- (1992)	$\bar{\nu}_e$
Strong	α (1896)	$^4_2$He
	n, p (1970), 2p (2000), 2n (2012)	n or p or 2p or 2n
	Cluster (1984)	^{14}C or ^{24}Ne or ^{32}Si, ...
	Fission (1939)	n's + 2 heavy nuclei
	Ternary fission (2010)	n's + 3 heavy nuclei

Table 5.1: Summary radioactive decays known today

5.2 Electromagnetic interaction decays

In the case of the gamma emission, the nucleus desexcites from an initial state of energy E_i towards a final state of energy E_f. The photon energy is to a good approximation

$$E = h\nu = E_f - E_i \tag{5.4}$$

The calculation of the gamma emission requires the electromagnetic transition operator, as showed by the Fermi golden rule (5.3). Considering the photon as a plane wave, the transition operator reads

$$\vec{r}e^{-i\vec{k}.\vec{r}'} \tag{5.5}$$

where k is the wave number of the photon. Expressing the exponential as a Taylor expansion, Eq. (5.5) generates r^ℓ terms with decreasing magnitude. The dominant term corresponds to ℓ=1. This is the so-called dipole electric transition (labelled E1). The next term corresponds to ℓ=2 (E2 transition), which is several orders of magnitude less probable than the E1 transition, etc. The typical mean-lifetime of nuclear excited states which desexcite by an E1 transition is about a few ps.

It should be noted that the conservation of both total angular momentum and parity by the electromagnetic transition is a necessary condition:

$$\vec{J_i} = \vec{J_f} + \vec{\ell} \qquad \pi_i\pi_f = (-1)^\ell \tag{5.6}$$

The nucleus has also a magnetic moment. It allows for so-called magnetic transition with the parity rule

$$\pi_i\pi_f = (-1)^{\ell+1} \tag{5.7}$$

The magnetic transitions are a bit less probable than the electric one because of the expression of the nuclear magnetic moment. In summary the most to the less probable gamma desexcitations are E1 > M1 > E2 > M2 > E3 > M3 ...

The internal conversion process corresponds to a desexcitation of the nucleus where the energy is directly transferred to an atomic electron (typically from the K-shell). The ejected electron with a typical 1 MeV energy will leave a hole which in turns generates X-ray emission when filled by another atomic electron.

5.3 Weak interaction decays

As in the electromagnetic case, the weak interaction is not intense enough to change the nucleonic structure of the nucleus, which is determined by the strong interaction. Therefore, by weak decay, the number of nucleons of the mother and daughter nuclei are identical. These are called isobaric transitions. As the weak interaction does not conserve isospin, it allows for the transformation of a proton into a neutron and vice-versa.

In vacuum, the proton is considered as a stable particle whereas the neutron β^- decays towards a proton with a mean lifetime of about 15 min. This is because the neutron mass is larger than the proton one (Q>0). But in a nucleus, Fig. 3.9 shows that the neutron and proton Fermi level can be either equal, or different, depending on the structure of the nucleus, but mainly on its relative number of protons (Z) and neutrons (N). For instance, if the proton Fermi level is larger than the neutron one then the proton may β^+ decay into a neutron. The weak interaction therefore regulates the large proton or neutron excess. If the neutron and proton Fermi levels are equal, the nucleus is stable with respect to weak decay. One can understand that this specific case encompasses a minority of nuclei (about 300, see section 3.5). The mean lifetime of weak decays can therefore be as small as a few ns or as large as a few days.

The β^- decay correspond to the reaction

$$ {}^A_Z X \rightarrow {}^A_{Z+1} Y + e^- + \bar{\nu}_e \tag{5.8} $$

and the necessary positive Q-value condition reads

$$ Q = m(A,Z)c^2 - m(A,Z+1)c^2 - m_e c^2 > 0 \tag{5.9} $$

The β^+ decay correspond to the reaction

$$ {}^A_Z X \rightarrow {}^A_{Z-1} Y + e^+ + \nu_e \tag{5.10} $$

and the necessary positive Q-value condition reads

$$ Q = m(A,Z)c^2 - m(A,Z-1)c^2 - m_e c^2 > 0 \tag{5.11} $$

The electron capture correspond to the reaction

$$ {}^A_Z X + e^- \rightarrow {}^A_{Z-1} Y + \nu_e \tag{5.12} $$

and the necessary positive Q-value condition reads

$$ Q = m(A,Z)c^2 + m_e c^2 - m(A,Z-1)c^2 > 0 \tag{5.13} $$

The calculation of the transition probabilities also uses the Fermi golden rule (5.3). In this case one needs i) the wavefunctions of the outgoing leptons, ii) the expression of the weak transition operator and iii) the overlap of the initial and final nuclear wavefunctions. In a simple approach, ii) can be approximated by a constant. Planes waves expansion for the electron and the neutrino are used which will generate a hierarchy of the transitions, named: allowed, first forbidden, etc. Moreover the (electron/neutrino) pair can have two total spin states: S=0 is called the Fermi transition and S=1 the Gamow-Teller one. These two types of transition have the same order of magnitude.

It should be noted that the β decay is at the origin of the neutrino discovery (3-body decay) and is still used as a major way to produce and study neutrino properties such as its mass or flavour oscillations.

5.4 Strong interaction decays

Strong interaction decays correspond to nucleons or groups of nucleons emitted by the mother nucleus: one neutron, one proton, 2 protons, alpha particle, clusters, until fission which can be considered as an extreme case of nucleonic radioactivity. Strong decay radioactivities rather exhibit a continuum of possible mass of emitted fragments: A=1,2,4,14,24,25,28,30,32,90,132.

The emission of one nucleon is possible if the corresponding Fermi level is larger than the edge of the confining potential. In that case the mean-lifetime is typically the time corresponding to the mass of the meson mediator of the strong interaction:

$$\tau = \frac{\hbar}{m_0 c^2} \simeq \frac{197}{140}.\frac{fm}{c} \simeq 10^{-23} s \tag{5.14}$$

This very short lifetime can be considerably increased by potential barriers such as the centrifugal one, or the Coulomb one in the case of protons: the tunnelling through the barrier impacts the lifetime. For instance ^{113}Cs is a proton emitter with a lifetime of the order of a μs.

The alpha decay plays a specific role: because of the spin and isospin symmetry (magic number N=Z=2) the alpha particle has a large binding energy (28 MeV). It can easily preform in the mother nucleus, before being emitted. This explains that is it the first radioactivity being discovered. It corresponds to the reaction

$$^{A}_{Z}X^{N} \rightarrow ^{A-4}_{Z-2}Y^{N-2} + ^{4}_{2}He \tag{5.15}$$

and the necessary positive Q-value condition reads

$$Q = m(A,Z)c^2 - m(A-4,Z-2)c^2 - m_\alpha c^2 > 0 \tag{5.16}$$

The alpha particle being much lighter than the daughter nuclei, it collects almost all the Q-value in its kinetic energy. This energy lies between 5 MeV and 10 MeV because of the large binding energy of the alpha particle.

The preformation of alphas into nuclei is related to cluster states discussed in Chapter 4. Fig. 5.1 shows the required excitation energy in order to break a nucleus into clusters such as alphas, ^{12}C, ^{16}O, etc.

Helped by shell effects, heavy nuclei can also emit heavier clusters than alphas. In 1985 the cluster radioactivity was discovered. Radium and Uranium isotopes can emit Ne or Mg clusters with a typical mean-lifetime of 10^{20} s. The daughter nucleus is usually the doubly magic ^{208}Pb nucleus.

Finally fission corresponds to the emission of such a large cluster that the daughter nucleus separates in two pieces. It should be noted that due to shell effect there is usually one fragment around A=132 and another one around A=90: the spontaneous fission is asymmetric.

5.5 The fluid analogy

As discussed in Chapter 3 the nucleon-nucleon interaction is attractive with a repulsive hard core at very short distance. Fig. 5.2 shows the superposition of this interaction with a typical in-

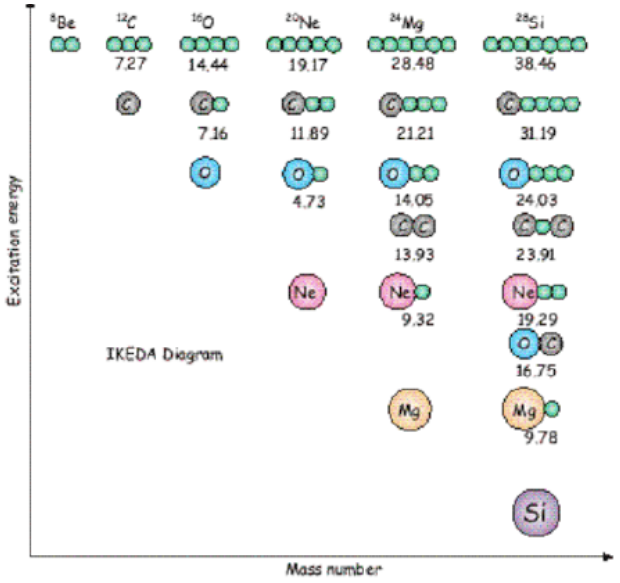

Figure 5.1: Ikeda diagram where nuclear states are displayed with cluster structure. The values (in MeV) are the excitation energy required to split the total nucleus into the corresponding clusters.

termolecular potential. The two interactions have a similar behavior. Since a system of molecules behaves as a fluid, such an analogy can be drawn in the nuclear case.

It is possible to consider the nucleus as a (quantum) liquid drop. Such an approach is complementary to the fully microscopic one based on the Dirac equation. The first one is easier but less predictive whereas the latter is more difficult to set up but is more predictive because it is based on fundamental principles such as the equation of motion.

One could therefore consider the nucleus as a fermionic charged superfluid quantum liquid drop. In that case its binding energy B (>0 if the nucleus is bound) reads

$$B = a_V A - a_S A^{2/3} - a_C \frac{Z^2}{A^{1/3}} - a_A \frac{(N-Z)^2}{A} + \delta \tag{5.17}$$

where the constants are

a_V=16 MeV

a_S=17 MeV

a_C=0,7 MeV

a_A=23 MeV

The first term is the attractive volume one, the second is the surface correction (where nucleons are less bound than in the volume of the nucleus), the third is the Coulomb repulsion among the protons, the fourth requires that neutrons and protons behave in a similar way, and the last term takes into account superfluidity: even-even nuclei are more bound than even-odd nuclei which are more bound than odd-odd nuclei because of pairing effect. Hence δ=12.$A^{-1/2}$MeV, 0 MeV and -12.$A^{-1/2}$MeV for even-even, odd-even and odd-odd nuclei, respectively.

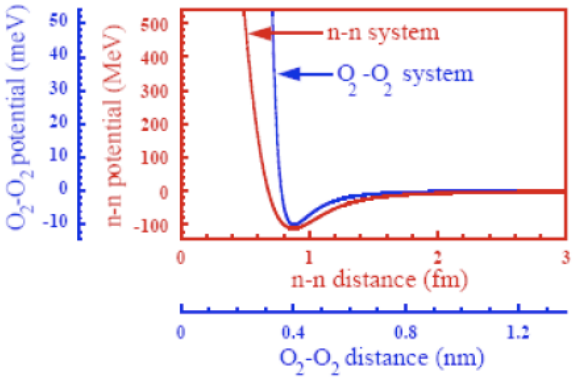

Figure 5.2: Comparison of the inter-nucleon and the inter-molecular potentials (from J. Dobaczewski, Joliot-Curie School 2002).

Eq. (5.17) is called the Bethe-Weizsäcker mass formula. It allows to calculate the mass mc^2 of the corresponding nucleus since

$$mc^2 = Zm_pc^2 + Nm_nc^2 - B \tag{5.18}$$

It also allows to discuss a relevant quantity, the binding energy per nucleon B/A, displayed on Fig. 5.3. The two main conclusions from this curve are i) at first order B/A is approximatively constant in nuclei: B/A $\sim$ 8 MeV and ii) in more details B/A exhibit a maximal value around A=56, meaning that nuclei in the ^{56}Fe vicinity are the most bound per nucleon. i) comes from the short range attractive + hard core strong interaction. ii) has important energetic consequences on fusion and fission processes on Earth and in stars: the fusion process is exoenergetic among light nuclei only until ^{56}Fe whereas the fission one is exoenergetic in heavy nuclei only down to ^{56}Fe.

Eq. (5.17) allows to understand the origin of the fission process. To fission a nucleus needs to deform. Therefore two opposite trends are at work: the Coulomb repulsion helps fission whereas the surface effect wants to minimise the surface and to keep the nucleus spherical, away from the fission. Therefore a nucleus can fission if

$$a\frac{Z^2}{A^{1/3}} > bA^{2/3} \tag{5.19}$$

where a and b are non-trivial constants depending on the liquid drop parameters described above. A deformed liquid drop needs to be considered in order to derive the expression of a and b.

Eq. (5.19) leads to

$$\frac{Z^2}{A} > \gamma = \frac{2a_S}{a_C} \simeq 50 \tag{5.20}$$

Z^2/A is called the fissility parameter. The larger value (above a few tens), the shorter the fission life time. The threshold value of the fissility parameter is rather 35 than 50. This shows

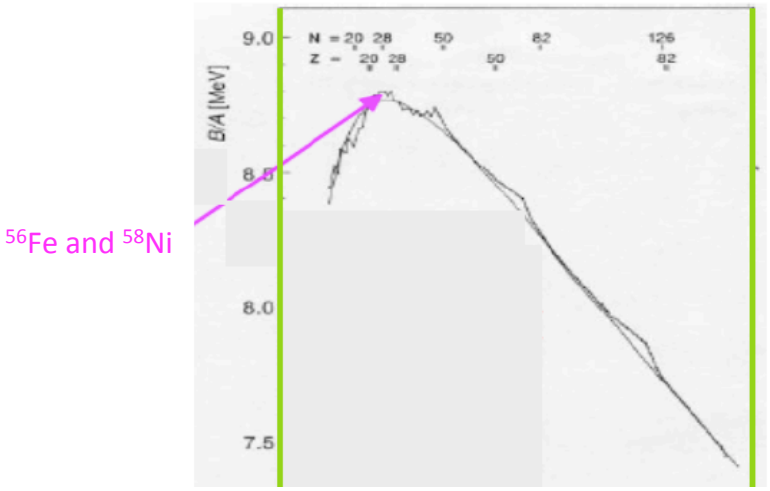

Figure 5.3: B/A as a function of A from the liquid drop formula.

that the liquid drop formula is useful to have a first idea of nuclear phenomenon but is not the ultimate nuclear approach. The typical fission lifetime lies between 10^{20} years and a μs for fissility parameter between 35 and 42, respectively.

Eq. (5.17) is also useful to better understand radioactive decays. Together with Eq. (5.18) one gets for the nuclear mass

$$mc^2 = \alpha + \beta Z + \gamma Z^2 \tag{5.21}$$

with

$$\alpha = A(m_n c^2 - a_V + a_A) + a_S A^{2/3} + \delta \tag{5.22}$$

$$\beta = m_p c^2 - m_n c^2 - 4a_A \tag{5.23}$$

$$\gamma = \frac{a_c}{A^{1/3}} + \frac{4a_A}{A} \tag{5.24}$$

For constant A, like in isobaric weak decay, the mass of the nuclei belongs to a parabola. Because of the δ value in Eq. (5.22), there is one parabola in the case of decays odd-even nuclei, and 2 parabolas in the case of decays among even-even and odd-odd nuclei. These 2 last parabolas are shifted by a $24A^{-1/2}$ value.

Eq. (5.21) also allows to predict the minimum of the parabola, namely the stable nucleus with respect to weak decay:

$$\left.\frac{\partial m}{\partial Z}\right|_{A=cst} = 0 = \beta + 2\gamma Z \tag{5.25}$$

leads to

$$Z \simeq \frac{A}{2 + (a_C/2a_A)A^{2/3}} = \frac{A}{2 + 0,015A^{2/3}} \tag{5.26}$$

One sees that light stable nuclei have N=Z=A/2 whereas for heavier nuclei (A $>$ 50) Z$<$A/2: stable nuclei are neutron-rich, such as ^{208}Pb.

Finally the alpha emitters region can also be pinned down using the liquid drop formula. The Q-value reads

$$Q = B(\alpha) - (B(X) - B(Y)) = B(\alpha) - \delta B \tag{5.27}$$

which becomes

$$Q = 28,3 - \frac{\partial B}{\partial Z}\delta Z - \frac{\partial B}{\partial A}\delta A \simeq 28,3 - 2\frac{\partial B}{\partial Z} - 4\frac{\partial B}{\partial A} \tag{5.28}$$

using Eq. (5.17) to evaluate the binding energy derivatives. One gets

$$Q = 28,3 - 4a_V + \frac{8a_S}{3A^{1/3}} + \frac{4a_C Z(3A - Z)}{3A^{4/3}} - 4a_A\left(1 - \frac{2Z}{A}\right)^2 \tag{5.29}$$

The numerical resolution of this equation using Eq. (5.26) gives Q $>$0 for A $>$ 150. Therefore heavy nuclei is a necessary condition in order to have alpha decay so that both the Coulomb and and surface terms favor the emission of the alpha particle.

Finally it should be noted that the fluid analogy can be extended to infinite nuclear matter. Nuclear matter can exist in sufficiently large nuclear systems such as neutron stars or heavy ion collisions. In this case a phase diagram can be predicted as displayed on Fig. 5.4. A superfluid to normal phase transition is also expected in nuclei for temperatures above 1 MeV. However nuclei are finite systems, and thermodynamical quantities should be considered with caution.

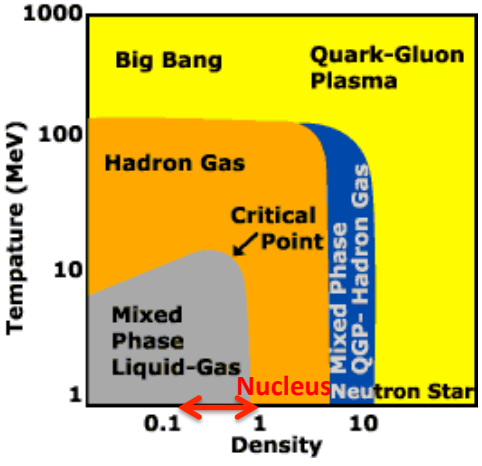

Figure 5.4: Phase diagram of nuclear matter. The density is given in units of the saturation density (0.16 fm^{-3}).

Fission and fusion

There are several types of fission:

- spontaneous fission
- induced fission by a slow neutron (kinetic energy $\sim 10^{-2}$ eV)
- induced fission by a fast neutron (kinetic energy ~ 1 MeV)
- induced fission by a very fast neutron (kinetic energy $\gtrsim$ few MeV)

The spontaneous fission has been discussed above (Eq. 5.19), and corresponds to tunneling effect through the fission bareer, with half-lives from ms to 10^{20} years.

In the case of the fission induced by a slow (also called thermal) neutron, there are only 7 so-called fissile nuclei ($^{233}_{92}$U, $^{235}_{92}$U, $^{239}_{94}$Pu, $^{241}_{94}$Pu, $^{230}_{91}$Pa, $^{236}_{93}$Np, $^{242}_{95}$Am). Each of these 7 nuclei has an odd number of neutrons. It allows to provide enough energy to overcome the fission bareer, by capturing the incoming neutron, so to build a neutron pair.

In the case of fission induced by a fast neutron, the same odd-even effect occurs. However, the neutron capture cross-section is about 3 orders of magnitude lower than the one for slow neutron. Hence, there is a non-negligible branching ratio of fast neutron capture which is not leading fission.

In the case of fission induced by a very fast neutron, its kinetic energy usually allows to overcome the fission bareer, and there are several dozens of nuclei which can fission after capturing such a neutron.

In a nuclear power plant, there are five main items to consider:

- the nuclear fuel
- the coolant
- the neutron moderator
- the control rods
- the nuclear wastes

The nuclear fuel is usually the ^{235}U fissile nucleus, coming from natural Uranium (0.7 %). 2 or 3 fast neutrons are also emitted during the fission. It is therefore necessary to slow these neutrons, in order to increase the neutron capture cross section by several orders of magnitude and generate the next fission in another nucleus. On this purpose, a neutron moderator is used, which can be water. Water can also play the role of coolant, to bring the generated heat towards the steam generator, in order for turbines to rotate. Finally, control rods can capture neutrons in order to maintain the chain reaction without any divergence. It should be noted that since Hydrogen of water can capture neutron, this parasitic effect has to be either compensated by enriching the fuel up to 3 % of ^{235}U, or eliminated by replacing Hydrogen of water by deuterium (use of so-called heavy water).

Nuclear wastes are the main drawback of nuclear power plants: the daughter nuclei from the fission are usually β^- emitters, with very different half-lifes and chemical composition (Z-value). The implications are twofold: i) even when the chain reaction is stopped, the daughter nuclei have to be cooled down, since they keep on releasing energy, due to their positive Q_β-values. ii) some of the nuclear wastes have very long half-lives, such as several millions years. They have to be stored or transmuted, but there isn't a clear solution emerging for now.

It is also possible to consider a fast neutron reactor. In this case, the low neutron capture cross section is compensated by the regeneration of fissile nuclei, thanks to the fast neutron capture. For instance, the following chain:

$$^{238}_{92}U + n \rightarrow ^{239}_{92}U \xrightarrow{\beta^-} ^{239}_{93}Np \xrightarrow{\beta^-} ^{239}_{94}Pu \tag{5.30}$$

allows to make a fast reactor work, where ^{238}U is the fertile nucleus, and ^{239}Pu the fissile one. A fast neutron reactor does not need any moderator. It could also be coupled to an accelerator to transmute nuclear wastes. All these systems, based on fast neutrons, are currently prototypes.

Controlled fusion requires temperature of 10^8 K (10 keV), in order to trigger enough reactions through the Coulomb bareer. This can be reached by two methods:

- inertial fusion
- magnetic confinement

In the inertial fusion, a strong compression of a deuterium-tritium mix is obtained using high-power lasers. In the magnetic confinement, the deuterium-tritium plasma is electromagnetically heated, while the magnetic field avoids any cooling contact with any surface.

Chapter 6

Probing nuclei

The only way to get experimental information on a nuclear state is either to detect its radioactive production or to perform a reaction on the corresponding nucleus.

When a reaction is performed two types of quantities can be measured: i) the kinematical quantities (energy, scattering angle) and ii) the number of relevant events. i) is used to order the types of events (elastic or inelastic scattering, etc.) unless one wants to test the validity of the special relativity. ii) leads to the measurement of the reaction probability (the cross section). This is directly related to Eq. (5.1) which is the quantity of interest because it provides informations on the interaction V_{int} responsible for the reaction or the structure (Ψ_i or Ψ_f) or the nucleus. Of course the kinematics of a reaction is also important in order to evaluate its feasibility.

6.1 Kinematics and reactions

Nuclear reactions are induced using an accelerated beam. Starting from the second Newton's law (in the special relativity framework) a particle (nucleus) with momentum p, charge q in a magnetic field B obeys to

$$\frac{dp}{dt} = \gamma m \frac{v^2}{R} = qvB \tag{6.1}$$

which can be rewritten as a fundamental law for accelerated beams:

$$BR = \frac{p}{q} = \gamma \frac{mv}{q} \tag{6.2}$$

The left hand side are typical accelerator features: its magnetic field B and its curvature radius R. The right hand side are properties of the particle (nucleus): mass m, velocity v and charge q.

Considering a reaction:

$$1 + 2 \rightarrow 3 + 4 \tag{6.3}$$

where 1 and 2 are the initial nuclei, and 3 and 4 the final ones, some conservation laws are in order. The total energy and momentum are conserved:

$$E_1 + E_2 = E_3 + E_4 \tag{6.4}$$

$$\vec{p_1} + \vec{p_2} = \vec{p_3} + \vec{p_4} \tag{6.5}$$

as well as the total angular momentum, including the relative orbital effect:

$$\vec{J_1} + \vec{J_2} + \vec{L_i} = \vec{J_2} + \vec{J_3} + \vec{L_f} \tag{6.6}$$

The electrical charge is also conserved:

$$q_1 + q_2 = q_3 + q_4 \tag{6.7}$$

as well as the baryonic number

$$B_1 + B_2 = B_3 + B_4 \tag{6.8}$$

If the nuclear reaction (or decay) occurs with the strong interaction, the isospin is conserved:

$$\vec{T_1} + \vec{T_2} = \vec{T_3} + \vec{T_4} \tag{6.9}$$

$$T_{31} + T_{32} = T_{33} + T_{34} \tag{6.10}$$

as well as the parity

$$\pi_1.\pi_2.(-1)^{L_i} = \pi_3.\pi_4.(-1)^{L_f} \tag{6.11}$$

In the case of the weak interaction none of Eqs (6.9,6.10,6.11) is conserved whereas the electromagnetic interaction allows for the conservation of the parity (6.11) and the projection of the isospin (6.10) (related to the charge conservation).

There are usually two types of reactions: i) the laboratory frame coincides with the the center of mass frame and ii) the laboratory frame is of the fixed target type. i) corresponds to cases where $\vec{p_1}$=-$\vec{p_2}$ in the laboratory (symmetric beams) since the center of mass frame is defined by

$$\sum \vec{p} = \vec{0} \tag{6.12}$$

both in the entrance and the exit channels.

ii) corresponds to the case of a beam sent on a fixed target: $\vec{p_2}$=0. It requires only one accelerator compared to case i), but the energy available for the reaction is less important since the laboratory frame does not coincide with the center of mass one.

If the Q-value is positive, the reaction is exothermic. If Q<0 kinetic energy has to be provided in the entrance channel in order to perform the reaction. The threshold energy T_S is defined as the minimal required kinetic energy in the entrance channel to produce the particle (nuclei) of interest in the exit channel. In the limit case where the output particles have no kinetic energy, the relativist invariant reads

$$I = \left(\sum E\right)^2 - \left(\sum \vec{p}c\right)^2 = \left(\sum_f m_f c^2\right)^2 \tag{6.13}$$

Using this expression the threshold energy is T_S=-Q/2 for each beam in case i) and

$$T_S = -\frac{Q}{2}\frac{\sum_{if} m_{if}c^2}{m_2 c^2} \tag{6.14}$$

for the beam (particle 1) in case ii).

The threshold energy is therefore minimal when the laboratory and the center of mass frames coincide as expected.

6.2 Cross sections and reactions

The cross section is an important quantity because it provides information of the interaction and/or the nuclear structure as stated above. In a nuclear reaction one should therefore know how to relate the number of relevant event n_0 per second to the cross section.

Considering a beam of intensity Φ particle per second irradiating a target of thickness e and with N nuclei per unit of volume, one gets

$$n_0 = \Phi(Ne)\sigma \tag{6.15}$$

where the proportionality constant σ is the interaction probability of one incident nucleus with one target nucleus. Eq. (6.15) shows that it is homogeneous to a surface and it is called cross section.

From a microscopic point of view, σ is directly related to Eq. (5.1). To grasp an order of magnitude of σ one could use a simple geometrical picture for the reaction:

$$\sigma \simeq \pi(R_1 + R_2)^2 \tag{6.16}$$

where R_1 and R_2 are the incident and target nucleus radii, respectively. Nuclei having typical radii of a few Fermis, σ is about 10^{-28} m^2. An useful unit is the barn defined as 1b$\equiv 10^{-28}$ m^2.

One could evaluate the order of magnitude of n_0/Φ, which is the rate of nuclei in the beam which interact with the target. The number of target nuclei per unit of volume is

$$N = \frac{\rho}{A}\mathcal{N} \tag{6.17}$$

where ρ is the target density and $\mathcal{N}$ the Avogadro number. N is typically 10^{21} nuclei per cm^3 for a nucleus with a few dozens of nucleons A. In a typical target of 30 μm thick, Eq. (6.15) gives:

$$\frac{n_0}{\Phi} \simeq 10^{-24}.10^{21}.30^{-4} \simeq 10^{-6} \tag{6.18}$$

Therefore only about one per one million of incident nuclei undergo a reaction with a nucleus of the target. This is due to the atomic structure of the target compared to the typical nuclear size and to the short range of the nuclear interaction.

Usually in experiment the events of interest are measured in a detector covering a solid angle dΩ. In this case the number of scattered nuclei impinging the detector per second is

$$dn_0 = \Phi(Ne)\frac{d\sigma}{d\Omega}d\Omega \tag{6.19}$$

where the proportionality constant is the differential cross section which measures the probability to scatter at the angle (θ,φ). Eqs. (6.15) and (6.19) yield

$$\sigma = \int \frac{d\sigma}{d\Omega}(\theta,\varphi)d\Omega = \int_0^{2\pi} d\varphi \int_0^{\pi} \frac{d\sigma}{d\Omega}(\theta)Sin\theta d\theta \tag{6.20}$$

Usually the system is rotationally symmetric around the Oz axis, therefore the φ dependence vanishes.

If the size of the detector is small compared to the target-detector distance d then the solid angle can be evaluated:

$$d\Omega = 4\pi\frac{S}{4\pi d^2} = \frac{S}{d^2} \tag{6.21}$$

In the case of a reaction driven by the electromagnetic interaction it is possible to calculate the differential cross section for the reaction between two point-like systems. This is the so-called Rutherford cross section:

$$\frac{d\sigma}{d\Omega} = \frac{\alpha^2}{16E^2 sin^4\frac{\theta}{2}} \tag{6.22}$$

where E is the kinetic energy of the (light) incoming beam.

Two effects can make the measured differential cross section differ from (6.22): i) the reaction can also occur with the strong interaction and ii) the target nucleus may not be a point-like system. i) happens for large scattering angles or also large beam energy, corresponding to small classical distance between the projectile and the target, below the range of the strong interaction. ii) allows to measure the nucleonic density of the target since as in the optical model, the differential cross section is related to the Fourier transform of the the shape of the target. Fig. 6.1 compares the Rutherford cross section (6.22) with the measurement of alpha particles on a Gold target. For alpha kinetic energies larger than 30 MeV the data disagree with the Rutherford cross section because of both strong interaction events and because the incident alpha becomes sensitive to the Gold nucleonic density. The experimental cross section gets smaller because the alpha can be captured without participating to the elastic scattering channel which is measured here.

Electron scattering on nuclei allows to measure the charge density of nuclei, showing the saturation effect (Fig. 3.4). Since lepton do not interact by the strong force, this allows for a clean measurement of the density of the nucleus.

6.3 Nuclear shapes and densities

Nuclei not always exhibit spherical shapes with saturation density in the bulk. It is the role of both the experiment and the theory to predict, measure and understand various effects, due to the large variety of phenomena occurring in nuclei, as explained in the introduction. For instance

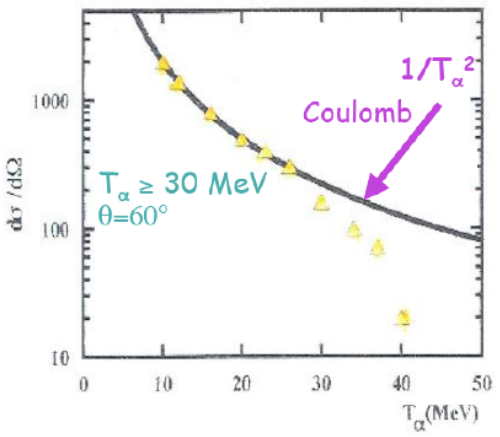

Figure 6.1: Elastic scattering cross section for the alpha+Au reaction as a function of the incident alpha kinetic energy.

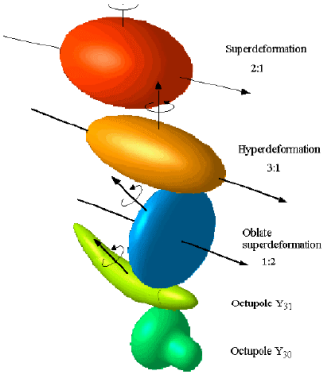

Figure 6.2: Various deformation of nuclear states

most of nuclei are not spherical but undergo spontaneous symmetry breaking, generating spatial deformation as depicted on Fig. 6.2

Some light nuclei like ^{11}Li exhibit an halo structure that is a very delocalised neutron wave-function as showed on Fig. 6.3. Finally various clusterised or even ring shapes are predicted as excited states of light N=Z nuclei (Fig. 6.4).

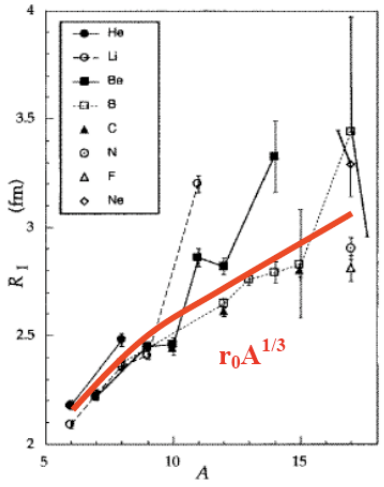

Figure 6.3: Measurement of radii in light nuclei.

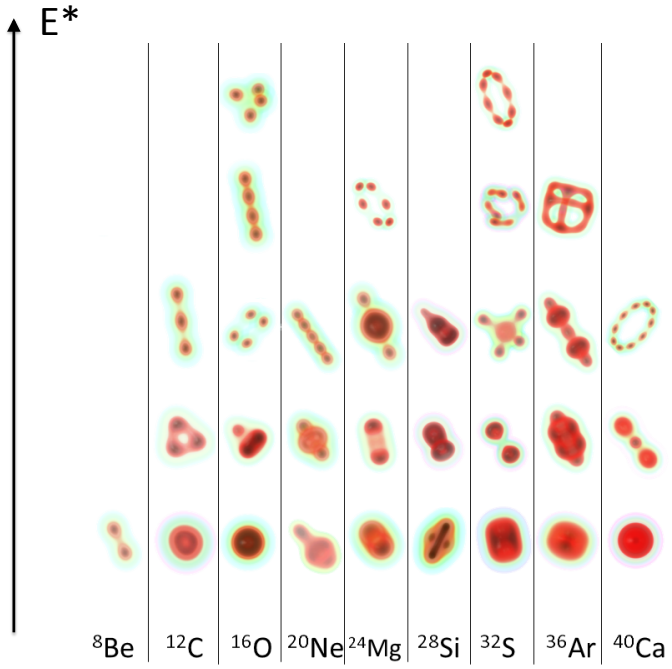

Figure 6.4: Nucleonic densities for various light N=Z nuclei predicted with the relativistic Dirac equation.

Chapter 7

Astronuclei

Nuclei are involved of several astrophysical processes. In order to understand these processes, nuclear structure inputs are in order. We shall here only mention them since they may be detailed in other courses. It should be noted that there is a corresponding nucleosynthesis for each astrophysical process described below, which shows the large variety of ways to produce nuclei in the Universe.

7.1 Nuclei in the Big-Bang

A few minutes after the Big-Bang the nucleosynthesis of light elements is triggered, and summarised on Fig. 7.1.

This primordial nucleosynthesis stalls around A=8 because of the very low cross section to produce the ^{12}C nucleus.

7.2 Nuclei in stars

Stars on their main sequence burn their hydrogen by fusion reactions. Because of the high temperature and large density (about 100 times larger than a few minutes after the big-bang) in a red giant environment, the following reaction becomes non-negligible:

$$\alpha + \alpha + \alpha \rightarrow^{12} C^* \rightarrow^{12} C + \gamma \tag{7.1}$$

This allows for Carbon synthesis and paves the way for heavier elements synthesis by fusion reactions until ^{56}Fe is reached. Then no more exoenergetic reaction is possible and the star gravitationally collapses.

It should be noted that ^{26}Al is produced in Novae and asymptotic giant branch stars mainly through the reaction:

$$^{25}Mg + p \rightarrow^{26} Al + \gamma \tag{7.2}$$

During its weak interaction decays towards ^{26}Mg, a γ of energy 1.8 MeV is emitted and can be detected by several space missions.

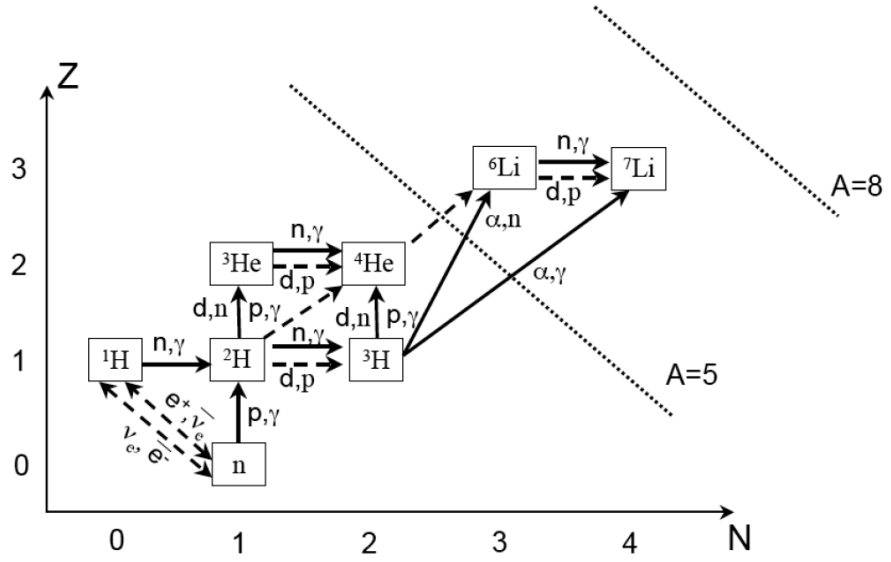

Figure 7.1: Reactions occurring during the primordial nucleosynthesis.

7.3 Nuclei in supernovae

If the star is massive enough, the collapse bounces because of the hard core of the nuclear interaction, generating a supernova. During this non-trivial event, electrons and neutrinos are captured by nuclei, modifying the proton over neutron ratio.

In the supernova explosion, some nuclei can also be irradiated by an intense neutron flux (the so-called r-process), rapidly increasing the neutron number of heavy nuclei. Weak decay allows then to transform excess neutrons into protons, leading to heavier elements than Iron.

7.4 Nuclei in cosmic rays

Nuclei may be accelerated in interstellar environment, becoming a component of cosmic rays. Some light nuclei undergo nuclear reactions such as the spallation one, which modify their abundances. This is a fourth type of nucleosynthesis in the Universe.

Nuclei are also possible candidates for Ultra High Energy Cosmic rays, having kinetic energies of typically 1 Joule. While propagating in the Universe, they emit nucleons by interacting with the Cosmic microwave background.

7.5 Nuclei-stars

Neutrons stars are the remnant of massive stars which went through core collapse supernovae. At first order they can be considered as a giant nuclei of 10 km size, around saturation density. In more details, the density of the star increases from 0.1 to several times the saturation density from the outer crust to the center of the star. Superfluid effects are expected to play an important role in their cooling. Neutron stars are indeed pulsars: they rotate while emitting electromagnetic waves.

Binary systems of neutron stars may also generates heavy elements due to the gravitational decompression of their crust. This is a fifth type of possible nucleosynthesis.